5101-81
Solar Thermal Power Systems Project
Research and Advanced Development

DOE/JPL-1060-44
Distribution Category UC-62

Evaluation of the Effects of a Freeze/Thaw Environment on Cellular Glass

P. Frickland
E. Cleland
T. Hasegawa

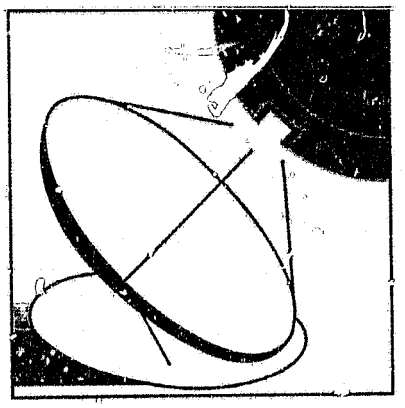

August 15, 1981

Prepared for
Solar Energy Research Institute
and U.S. Department of Energy
Through an agreement with
National Aeronautics and Space Administration
by
Jet Propulsion Laboratory
California Institute of Technology
Pasadena, California

(JPL PUBLICATION 81-29)

5101-81
Solar Thermal Power Systems Project
Research and Advanced Development

DOE/JPL-1060-44
Distribution Category UC-62

Evaluation of the Effects of a Freeze/Thaw Environment on Cellular Glass

P. Frickland
E. Cleland
T. Hasegawa

August 15, 1981

Prepared for
Solar Energy Research Institute
and U.S. Department of Energy
Through an agreement with
National Aeronautics and Space Administration
by
Jet Propulsion Laboratory
California Institute of Technology
Pasadena, California

(JPL PUBLICATION 81-29)

5101-81
Solar Thermal Power Systems Project
Research and Advanced Development

DOE/JPL-1060-44
Distribution Category UC-62

Evaluation of the Effects of a Freeze/Thaw Environment on Cellular Glass

P. Frickland
E. Cleland
T. Hasegawa

August 15, 1981

Prepared for
Solar Energy Research Institute
and U.S. Department of Energy
Through an agreement with
National Aeronautics and Space Administration
by
Jet Propulsion Laboratory
California Institute of Technology
Pasadena, California

(JPL PUBLICATION 81-29)

Prepared by the Jet Propulsion Laboratory, California Institute of Technology, for the U.S. Department of Energy through an agreement with the National Aeronautics and Space Administration.

The JPL Solar Thermal Power Systems Project is sponsored by the U.S. Department of Energy and forms a part of the Solar Thermal Program to develop low-cost solar thermal and electric power plants.

ABSTRACT

Cellular glass technology with respect to solar energy applications is briefly reviewed and current applications and related studies are discussed. Using the evaluation criteria of water vapor permeability and conformability, a protective butyl rubber/silicone conformal coating system was selected for use on Foamglas® substrates in a freeze/thaw environment. The selection of a specific freeze/thaw cycle which closely models field conditions is discussed. A sampling plan is described which allows independent evaluation of the effects of conformal coatings, cycle number and location within the environmental chamber. The results of visual examination, measurement of density, modulus of rupture and Young's modulus are reported. Based upon statistical evaluation of the experimental results, it was concluded that no degradation in mechanical properties of either coated or uncoated Foamglas® occurred within the duration of the test (53 freeze/thaw cycles). Recommendations are made for further work in the area of the effect of selected coatings on cellular glass in the freeze/thaw environment.

PREFACE

The purpose of this report is to document a definitive investigation of the freeze/thaw degradation of cellular glass. A cellular glass representative of those commercially available was studied under freeze/thaw conditions, with and without selected conformal coatings. Degradation was quantified by the determination of physical properties of the conditioned cellular glass as compared to control samples.

The work described herein was conducted by the Jet Propulsion Laboratory (JPL) of the California Institute of Technology, Section 354 (Applied Mechanics Technology) during the fiscal years 1980 and 1981. The freeze/thaw conditioning of test samples was conducted with the assistance of Section 357 (Test and Mechanical Support), also at JPL. This report documents the technical approach taken, the results, and the conclusions determined during the investigation. Recommendations for future work are also included.

ACKNOWLEDGMENT

Contributions to the study are acknowledged from the Applied Mechanics Technology Section, Applied Mechanics Division, Jet Propulsion Laboratory, California Institute of Technology as follows:

Dr. M. Adams
Mr. R. Bamford
Mr. R. Helms
Dr. J. Zwissler.

CONTENTS

Figures

Tables

SECTION I

INTRODUCTION

Cellular glass has been identified as a candidate for use as a structural substrate in second-surface glass mirror solar reflector designs. However, there exists widespread concern over the ability of the material to resist the severe environmental conditions (specifically high humidity combined with cyclic freeze/thaw temperature) which can be expected in field applications. Hence, the purpose of this report is to contribute to the technology of cellular glass for solar thermal applications by characterizing its degradation resistance to a known freeze/thaw environment.

In an effort to define the rate of freeze/thaw degradation in cellular glass, an environmental test plan was developed, and executed, and the results of the test matrix analyzed for significance. The test specimens used in the plan were fabricated from Pittsburgh Corning's Foamglas® standard insulation cellular glass which was chosen as being representative of typical commercially available cellular glass. At the heart of the test plan is a freeze/thaw cycle which is representative of the high humidity freeze/thaw conditions which would reasonably be expected for solar collector installations. This cycle was used to environmentally condition both bare Foamglas® blocks and Foamglas® blocks which had been coated with a highly moisture-resistant coating. The conditioned blocks were then tested against control blocks which were kept at 0% relative humidity (RH) and 30°C.

SECTION II

CELLULAR GLASS TECHNOLOGY

A. BACKGROUND

Since its development in the late 1930s, foamed cellular glass has been mainly used for commercial and industrial thermal insulation. The two types of cellular glass which are commercially available in large quantities are Foamglas®, a soda-lime silicate glass, and Foamsil-28®, a borosilicate glass. Both are produced by the Pittsburgh Corning Corporation (PCC), Pittsburgh, Pennsylvania. Foamglas® is available as both Standard Insulation Foamglas® and Foamglas® High-Load Bearing Insulation. The latter is select Foamglas® with higher compressive load bearing capability. Solaramics, Inc. of El Segundo, California also produces a soda-lime silicate foam, but in much lower quantities.

Recently, Foamglas® and Foamsil-75®, a developmental material, have been identified as two of several candidate materials for the structural mirror substrate of solar concentrators.[1] Specific properties which make these materials attractive for this application are their relative low cost, high stiffness-to-weight ratio, thermal expansion coefficient (which can match dense glass), chemical and dimensional stability, machinability and potential recyclability.[2] Typical properties of these materials are shown in Table 1. For a more complete discussion of specific materials' properties, consult the work of Giovan and Adams[1] and Zwissler.[3]

B. CURRENT SOLAR APPLICATIONS AND RELATED STUDIES OF CELLULAR GLASS

This section gives a brief history of the development and use of foamed cellular glass in structural applications. Its purpose is to provide a background and understanding in the development of the current cellular glass freeze/thaw controversy.

During the late 1940s, Pittsburgh Corning began marketing foamed cellular glass. Its major use was as roof, deck, wall and industrial insulation. The applications could not be considered truly structural; however the material was frequently required to support modest rooftop loads (personnel, light machinery, etc.). The cellular glass was generally, though not always, coated with asphalt, coal tar or membrane coverings and has been shown to retain its thermal properties over the years quite well.[4]

In 1974, Kaplar investigated the moisture absorption and freeze/thaw effects on cellular glass along with several other synthetic foamed materials. His conclusions were that although cellular glass exhibited very little moisture absorption in long-term immersion tests, it quickly deteriorated when subjected to freeze/thaw conditions while totally immersed in water (see Figure 1). This is the first report of a freeze/thaw evaluation of cellular glass while in a "high humidity" environment.

Table 1. Properties of Commercially Available Cellular Glass[1]

Material	Foamglas® (Standard)	Foamglas® (High Load Bearing)	Foamsil-28®
Density (lb/ft^3)	8.5	8.5	12
Modulus of Elasticity (x 10^5psi)	1.5	1.5	1.8
Average Flexure Strength (psi)**	80	80	[illegible]
Average Compressive Strength (psi)	75*	100*	210
Average Shear Strength (psi)	50	50	---
Coefficient of Thermal Expansion (x $10^{-6}/^oF$)	4.6	4.6	1.6
Dimensional Stability	Excellent	Excellent	Excellent
Cost ($/board foot)***	0.31	0.34	2.55

*Guaranteed average compressive strength
**Measured in three-point bend
***In millions of board feet, 1978 dollars

About the same time, PCC was recommending multiple asphalt and felt coatings for the protection of Foamglas® in a similar environment[5] (under the freeze slab of ice rinks).

The next known study which included cellular glass was by Argoud in the spring of 1975.[6] He submitted bare Foamglas® with mirrored glass bonded to it to approximately 400 freeze/thaw cycles (see Figure 2). Occasionally, throughout the cycle, water was manually poured onto the mirror surface. The bare edge of the Foamglas® was observed to partially spall away, resulting in a rounding off of the corners (see Figure 3). No major fractures or disbonding were observed; however, the retained mechanical strength of the material was not evaluated.

From 1976 to 1978, work began on two projects which used Foamglas® as a glass mirror substrate for a solar collector: the Test Bed Concentrator (TBC) at JPL (Argoud) and the Sunfire Project directed by F. Broyles (see Figures

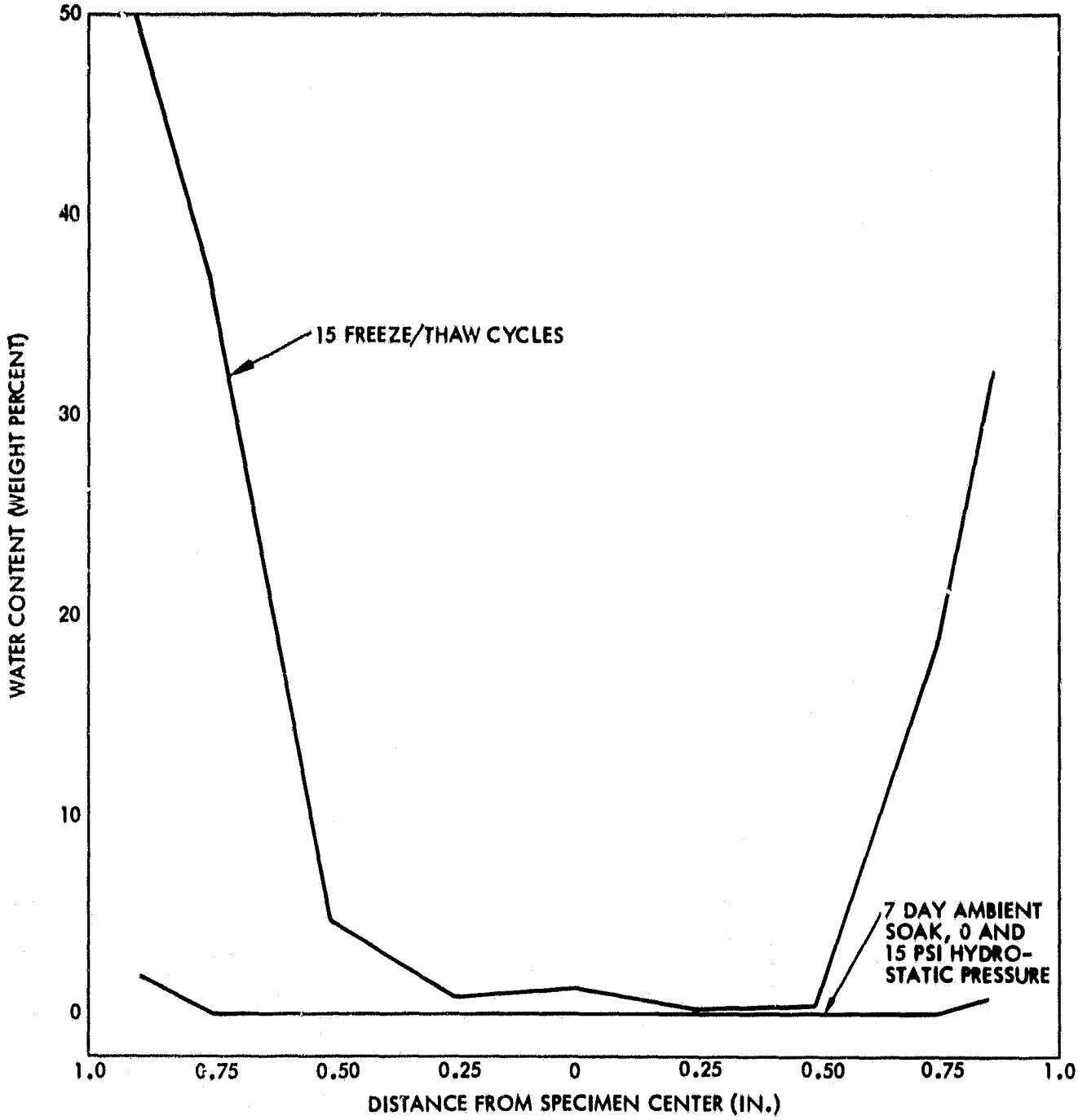

Figure 1. Summary of Results: Freeze/Thaw Tests Results for Cellular Glass (C.W. Kaplan, 1974)

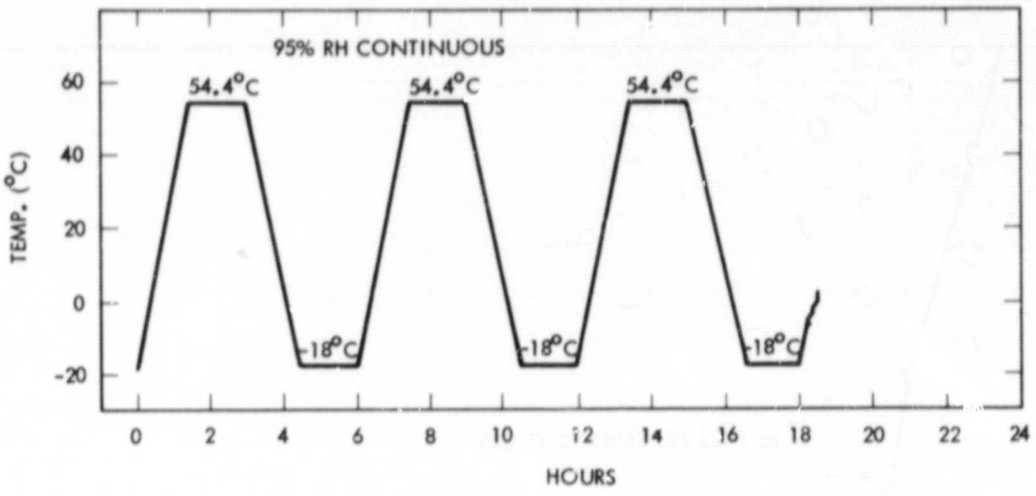

Figure 2. Freeze/Thaw Cycle (Argoud, 1975)

Figure 3. Foamglas® with Glass Mirror (Argoud)

4 and 5). The Sunfire Project used materials and processes which were basically adapted from the techniques developed by Argoud. A major difference was that the Sunfire reflective panels did not have a protective coating on the Foamglas®, whereas the TBC reflective panels ultimately did.

Figure 4. Test Bed Concentrator Reflector Panel.

To support the development of the TBC reflector elements (specifically in the area of the evaluation of mirror bonding techniques) Argoud initiated another freeze/thaw test of uncoated Foamglas /mirror glass specimens.(6, 7) The cycle is shown in Figure 6. At the conclusion of the 38-day test the Foamglas® appeared sound with some slight edge spalling noted (see Figure 7).

In August 1978, the first hard copy appeared concerning the design allowables for Foamglas® used as structural backing for mirror facets.(8) These engineering data were gathered to support the growing interest in using cellular glass materials in various point-focus solar collector programs at JPL.

Also in 1978, Sandia Laboratories Albuquerque (SLA) began considering Foamglas® while evaluating materials for use in their line-focus solar

Figure 5. Sunfire Project Concentrator

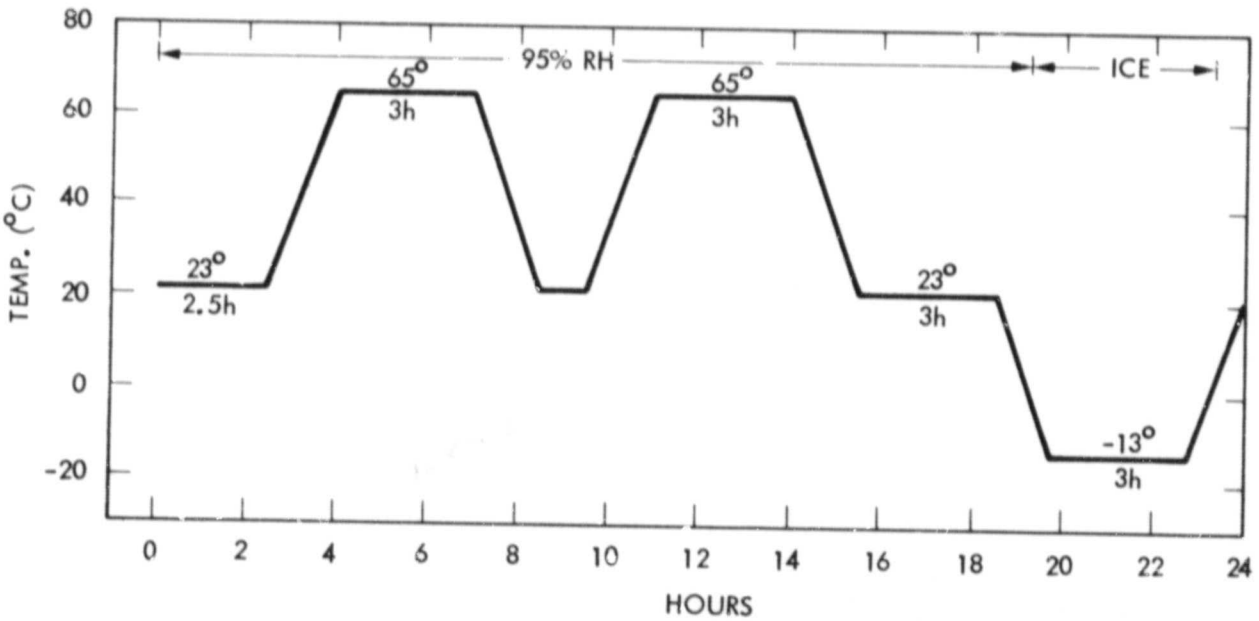

Figure 6. Freeze/Thaw Cycle (Argoud, 1978)

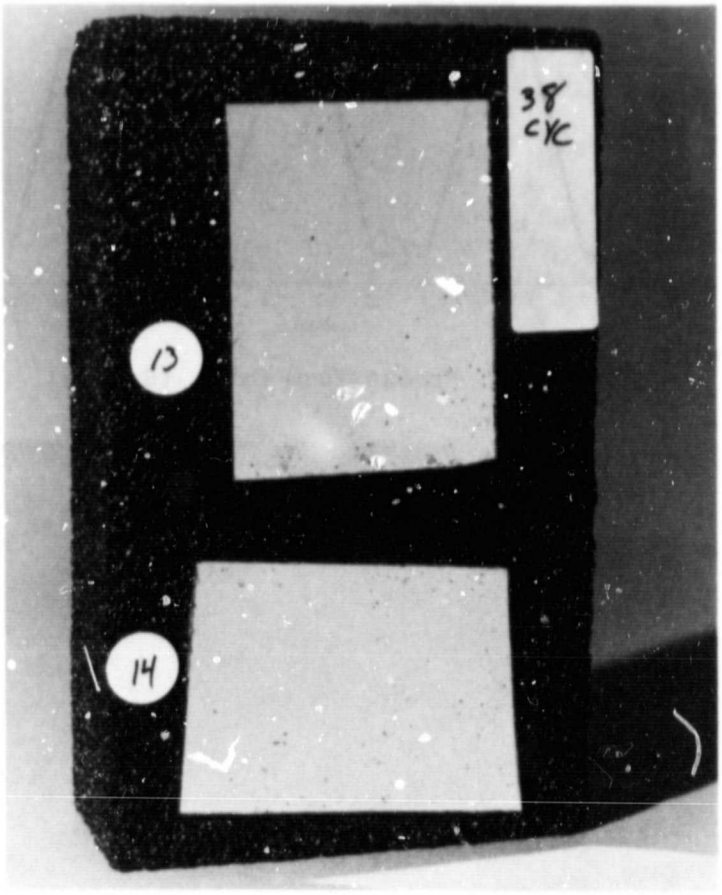

Figure 7. Foamglas® Mirror Adhesion Test (Argoud)

collectors. SLA studied both accelerated and real-time exposures of coated and uncoated Foamglas®, and Solaramics cellular glass.[6,9,10,11] The accelerated conditioning cycle, shown in Figure 8, was run for approximately 6 months and real-time outdoor exposure was accomplished on a local rooftop for 11 months. The cellular glass was observed to be especially sensitive to the freeze/thaw environment in all cases. It was postulated that water penetrated the coating, thereby causing delamination, which opened the surface to spalling followed by crack formation leading to catastrophic structural failure. Figure 9 is a photograph of one of the rooftop conditioned panels.

In an effort to determine whether a protective coating would provide a solution to the freeze/thaw problem, Allred initiated another test program. Various densities of Solaramics cellular glass blocks (approximately 2 inches by 4 inches by 8 inches) were given very thick (possibly up to 0.125 inch) coatings of silicone, polysulfide and urethane sealants. After more than a year of conditioning with the same cycle previously used, no degradation was noted. In the evaluations, one coating did allow a significant weight gain due to absorbed water content; however the other two appeared to resist significant water penetration.[11]

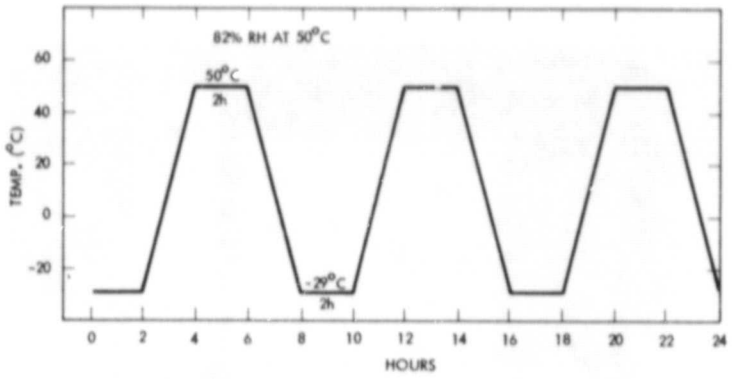

Figure 8. Freeze/Thaw Cycle (Sandia)

Figure 9. Degraded Glass/Cellular Glass Panel (Sandia)

After learning of the SLA results, Giovan and Argoud initiated another set of environmental freeze/thaw tests which evaluated coated and uncoated Foamglas® and Foamsil® and an uncoated sample of Solaramics cellular glass. The environmental exposure cycle which was used is shown in Figure 10.

A catastrophic failure of uncoated Foamglas® was noted after 42 cycles. The Foamsil® samples showed less effect at this time and coated Foamglas® appeared to be unaffected. The Foamsil® samples, plus additional Foamglas® samples, were returned to the chamber for an additional 101 cycles. The uncoated Foamsil® failed catastrophically, the coated Foamglas® still appeared unaffected and the uncoated Solaramics samples exhibited a weight gain of approximately 120%, yet still appeared structurally sound[6] (see Figure 11). The weathered specimens (Figures 12 and 13) exhibited surface spalling, crack formation, layered exfoliation and chemical leaching (color variations).

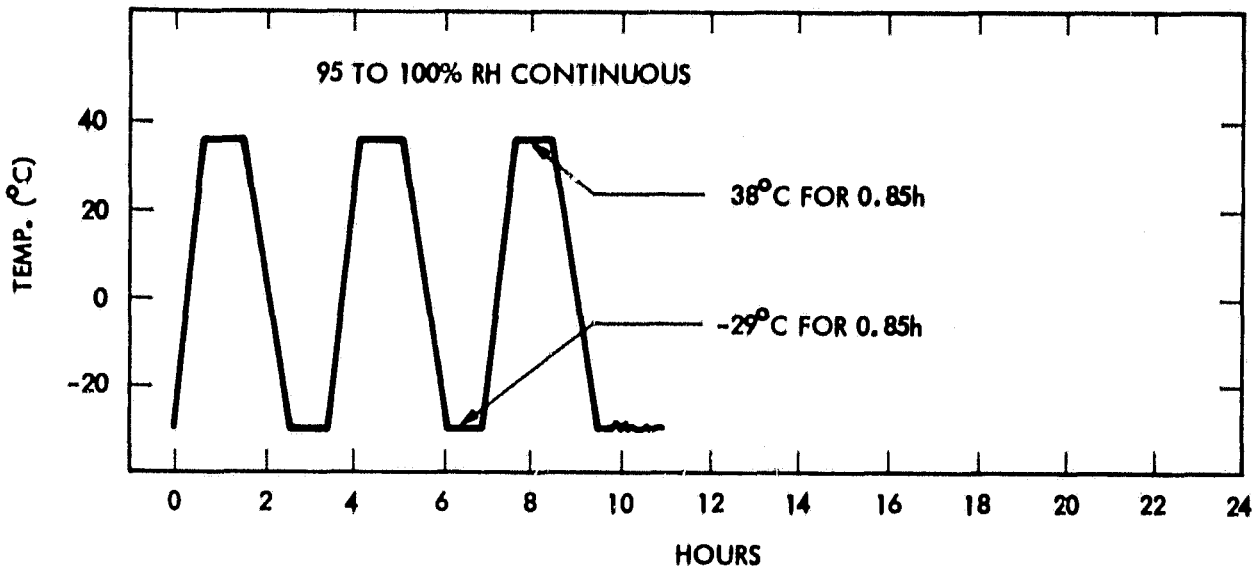

Figure 10. Freeze/Thaw Cycle (Giovan & Adams)

Although the data seemed to be somewhat conflicting, it appeared that coatings could have a significant impact on the weatherability of the cellular glass. This prompted Cleland and Carpenter at JPL to begin a broad evaluation of conformal coatings for cellular glass.(12) This early work provided the beginnings of what ultimately evolved into the coatings approach for this report.

In May of 1979, Giovan issued a report discussing the freeze/thaw sensitivity of Foamglas when used with and without a conformal coating. Because this report was specifically generated to support solar concentrator development work at JPL, it dealt with application- and design-specific recommendations for improving the weatherability of the TBC mirror facets. The general conclusions were that unprotected Foamglas® degraded in the freeze/thaw environment and that specific coatings increased the resistance of Foamglas® to weathering, although long-term coating durability was questionable.(13)

Shortly thereafter, Hasegawa issued a report on the failure analysis of mirrored Foamglas® panels which were coated and in some cases included mirror edge sealant(14). These panels were conditioned by Argoud (JPL) using the cycle previously shown in Figure 6. The specimens were cycled while in a vertical orientation within the test chamber. The complete degradation of Foamglas® in the presence of puddled water, and the apparent mechanical failure at the interface of cellular glass in contact with the mirror backing, was observed.

At this same time (June 1979) Giovan and Adams published a compilation of much of the recent work completed at JPL dealing with structural cellular

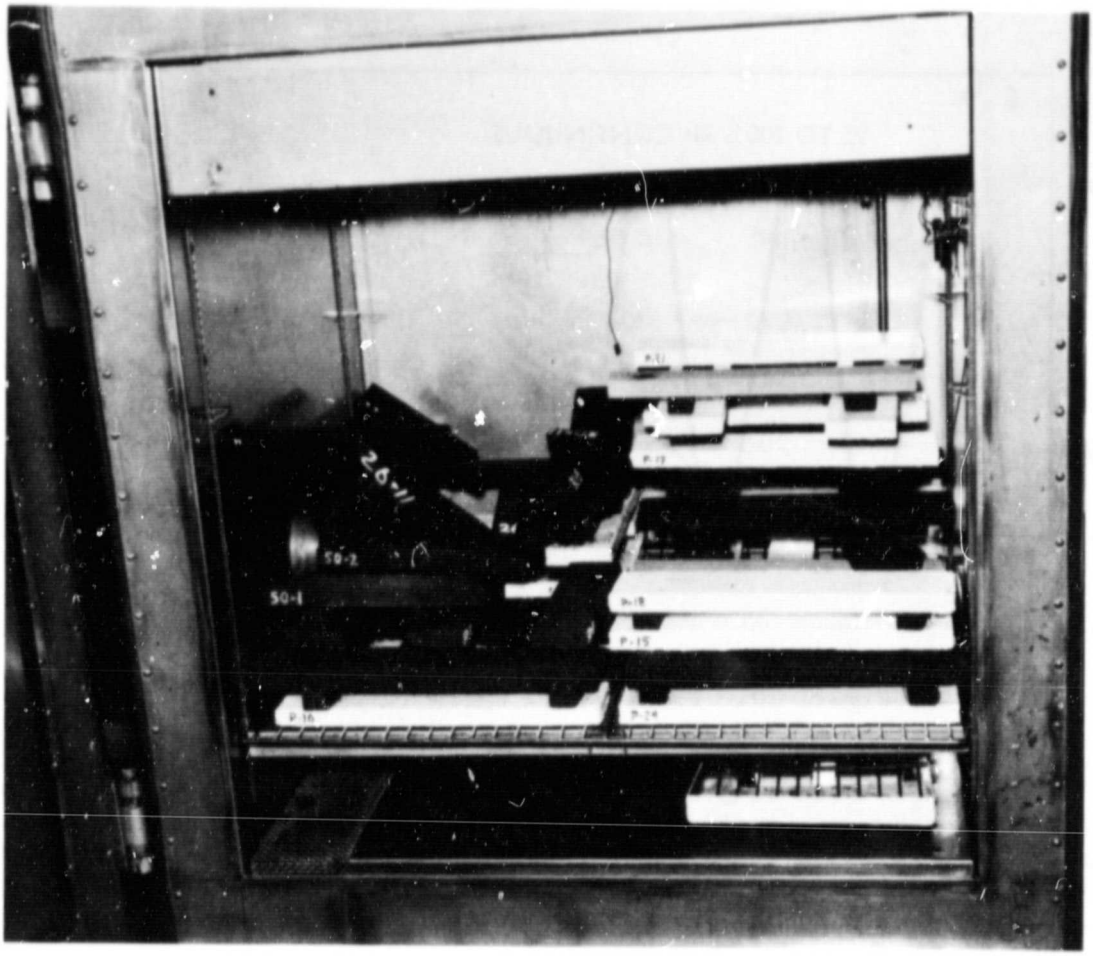

Figure 11. Coated and Uncoated Cellular Glass Blocks (JPL)

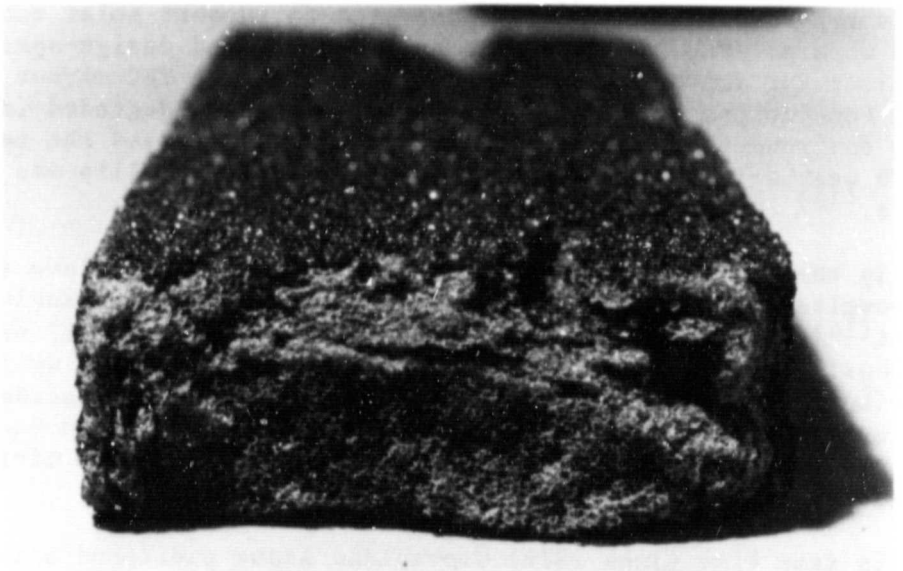

Figure 12. Degraded Cellular Glass

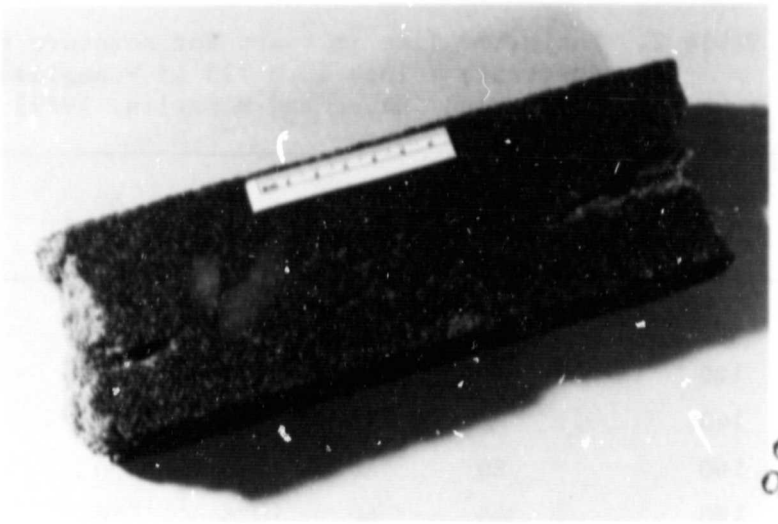

Figure 13. Degraded Cellular Glass

glass applications in solar concentrators.[1] This is currently the most complete published work on the structural and physical characteristics of cellular glasses.

In September 1979, McMarlin at PCC issued a technical information letter[15] which discussed the potential of freeze/thaw degradation of cellular glass. The letter indicated that damage could be expected to occur if water is confined inside cellular spaces or joints, whereas little damage would be expected on vertical surfaces where water can drain off.

Later that same month McMarlin and Meyer (PCC) issued another technical information letter[16], this time discussing the durability of Foamglas® in an aqueous environment. Based on powder solubility and hydroclave tests, the penetration of water at various temperatures and humidities was discussed and diffusion rates were calculated to be extremely low[17] (see Table 2).

The conclusions stated in these and other PCC bulletins were corroborated by a PCC study[18] of 20-year-old Foamglas® which was used as industrial tank insulation. Although the Foamglas® was completely exposed (unprotected) to the environment in Emlenton, PA, virtually no change in density or thermal conductivity (indicating no water penetration) was observed.

While supporting heliostat development early in 1980, Berry at Boeing Engineering and Construction Company, conducted freeze/thaw tests of Foamsil® which had solid glass face sheets and in some cases edge coatings.[19] The 8-hour cycle which was used is shown in Figure 14. After about 100 cycles the coated samples experienced a very slight weight loss and the uncoated samples exhibited about a 1% weight gain accompanied by very slight surface spalling. No fractures were noted.

Table 2. Estimated Time in Years for Moisture to Penetrate 1 Inch into 733 AJ Foamglas® Insulation (Meyer and McMarlin, 1979)

°F	20	40	60	80	100
			Relative Humdity (%)		
100	--	--	--	50	20
120	--	--	50	40	15
140	--	50	40	30	10
160	80	45	40	20	5
180	45	40	25	10	3
200	40	20	10	5	2
220	35	15	8	2	0

Late in 1980, SLA published a report addressing the use of protective coatings and sealants for solar applications.[20] They found no degradation of cellular glass after a year of 3 freeze/thaw cycles per day (using the same cycle previously used by SLA) when it was coated with a styrene-butadiene copolymer (Kraton 1101).

Under a contract with JPL, Acurex Corporation is developing an advanced solar concentrator constructed of large paraboloidal glass mirror panels with contoured Foamglas® as the structural substrate material. The freeze/thaw test results from this program are not available at this time.

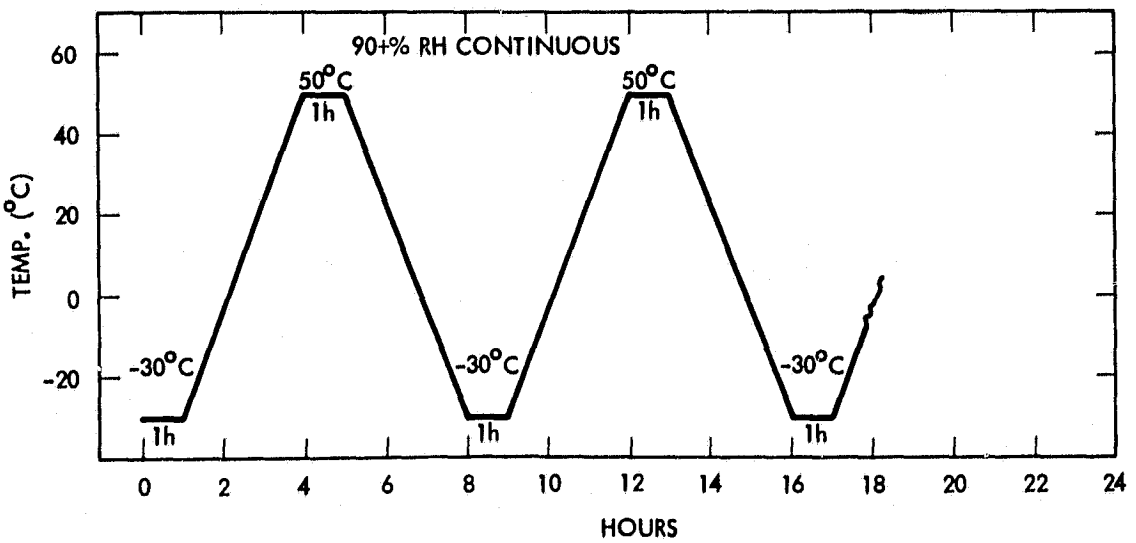

Figure 14. Freeze/Thaw Cycle (Boeing)

SECTION III

CONFORMAL COATINGS SELECTION

A. BACKGROUND

The conformal coatings used in this study were selected from an initial survey of candidate coating materials for cellular glass substrates.[12] Of 15 generic coating systems identified as having reasonable potential, nine individual and combined coating systems (Table 3) were evaluated to select a system with the potential to prove the feasibility of protecting cellular glass from the freeze/thaw environment. It should be emphasized that no attempt was made to identify the best commercial product for a given coating system.

B. EVALUATION CRITERIA

Two criteria were used in evaluating candidate conformal coatings. First, the ability of a coating to form a smooth surface was identified as crucial to coating performance. This was based on a study done in 1974 in which Kaplar[21] reported that severe freeze/thaw degradation occurs in cellular glass when the water content of surface pores exceeds 90%. This was confirmed in 1979 by Giovan and Adams[1] when they observed catastrophic failure of uncoated cellular glass during repetitive cycling through 0°C in the presence of free-standing water on the surface.

The same study also indicated that conformal coating performance could be seriously compromised by discontinuities in the coating surface such as small pinholes.[22] Kaplar also reported on studies, conducted in Greenland, which reported that high water-vapor gradients within cellular glass joints caused cellular glass spalling. From this, the second criterion for selection of candidate coatings, namely the requirement for minimal water vapor permeability, was identified.

C. TEST PROCEDURE

The test used to evaluate coating performance was ASTM D 1653-72, "Moisture Vapor Permeability of Organic Coating Films." The samples were prepared on a Teflon sheet using brush coating techniques and a drying time of approximately 25 minutes was allowed between coats. The specific apparatus used was a Fisher/Payne Permeability Cup No. 13-338.

D. RESULTS

The results of the moisture permeability tests (Table 4) indicate that coating system #7, a butyl rubber/silicone system, is more effective with respect to both specific permeability and moisture transmission. This coating system was chosen for conformally coating the Foamglas® specimens.

Table 3. Candidate Conformal Coatings

Material	Mix ratio	Coats	Cure time* (hr)
Amercoat® 234	1 component	3	24
Amercoat® 383	A - 80 v/o** B - 20 v/o	2	24
Urafilm® 1-1C-5	1 component	3	24
Amercoat® 33	1 component	3	24
Amercoat® 5403	1 component	3	24
Butylite® 711	A - 88.2 w/o*** B - 11.8 w/o	2	24
Butylite® 711/ Amercoat® 5403	Butylite® (as above) Amercoat® (one component)	2 (Butylite®) 2 (Amercoat®)	24 24
Pittcote® 404	1 component	3	24
Pittcote® 404/ Chemglaze® II (A276)	1 component 1 component	3 (Pittcote®) 2 (Chemglaze®)	24 24

*At room temperature
**Volume percent
***Weight percent

Table 4. Moisture Permeability of Candidate Materials

Material	Coating thickness (millimeters)	Specific permeability(1) (milligrams)	Moisture transmission(2) (milligrams)
1) Amercoat® 234 (acrylic)	0.0635	0.2455	3.9
2) Amercoat® 383 (epoxy)	0.1524	0.3237	2.2
3) Urafilm® 1-1C-5 (polyurethane)	0.1270	0.2860	2.3
4) Amercoat® 33 (vinyl)	0.1651	0.4001	2.4
5) Amercoat® 5403 (silicone)	0.1397	0.3901	2.8
6) Butylite® 711 (butyl)	0.0889	0.2676	3.0
7) Butylite® 711/ Amercoat 5403 (butyl/silicone)	0.1270	0.1277	1.0
8) Pittcote® 404 (acrylic latex)	0.5588	8.438	15.1
9) Pittcote® 404/ Chemglaze II, A276 (acrylic/polyurethane)	0.6096	7.545	12.4

(1) Specific permeability: milligrams of water which permeated 1-millimeter thickness of 1-square-centimeter sample in 24 hours.

(2) Moisture transmission: milligrams of water transmitted through 1-square-centimeter of sample in 24 hours.

SECTION IV

SPECIMEN PREPARATION

A. BLOCK PREPARATION AND PRECONDITIONING

The Foamglas® billets were 5 by 18 by 24 inches when received. They were cut into 4- by 5- by 18-inch blocks to simplify the handling, coating and environmental conditioning procedures. Blocks were then stored for a minimum of 14 days at 30°C and 0% RH prior to coating. Those blocks which were not coated were stored in a similar manner until either conditioning or testing was initiated.

B. COATINGS APPLICATION

Two coats of both the butyl rubber and silicone coatings were applied to the cellular glass blocks using standard brushing techniques. All blocks were allowed to "dry" for 24 hours after each butyl coat and 18 hours after the first silicone coat. The second silicone coat was allowed to dry for 24 hours prior to beginning freeze/thaw conditioning.

Attempting to obtain a continuous butyl rubber coating resulted in some difficulties, manifested by film tensile failure in the cellular "valleys" (Figure 15) and on the cellular "ridges" (Figure 16). Both were postulated to

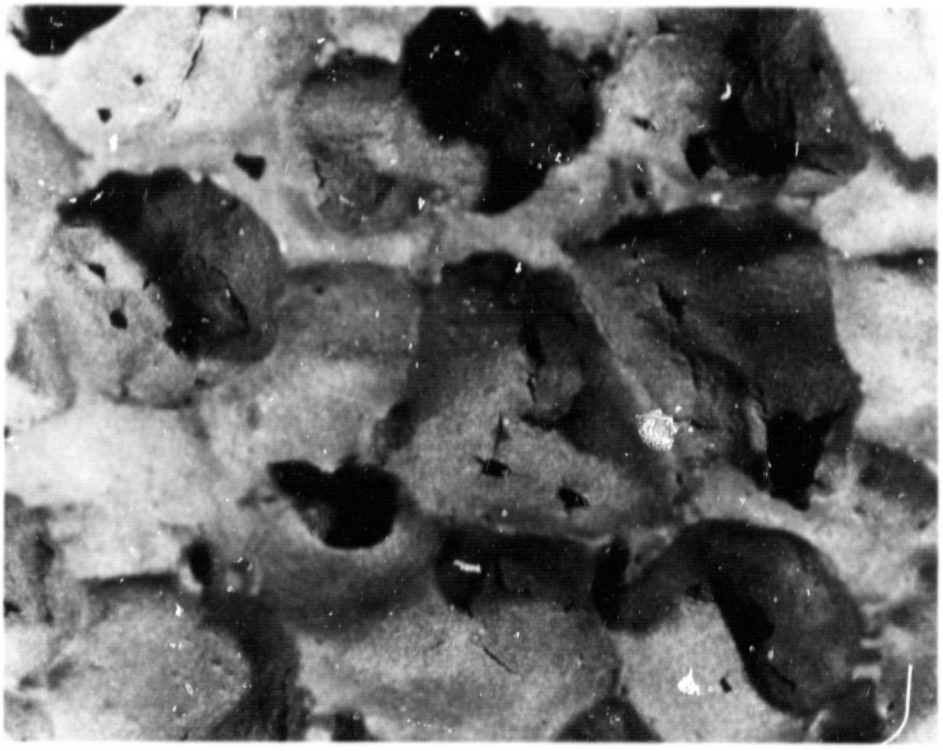

Figure 15. Cured Butyl Rubber Coating (One Coat)

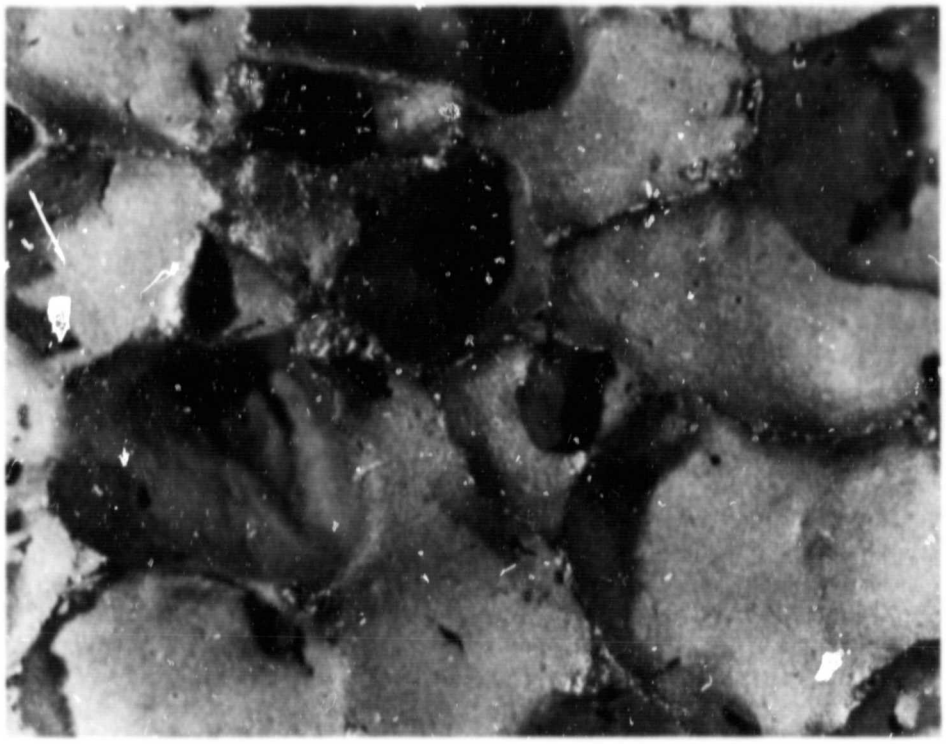

Figure 16. Cured Butyl Rubber Coating (One Coat)

be the result of shrinkage which occurred during solvent evaporation and polymerization. This problem may have been accentuated by the butyl rubber formulation, which contained a higher content of xylene solvent than that normally used for brush applications. The problem was lessened with the addition of a second coat of material (Figure 17). The remaining surface discontinuities were apparently sealed with the silicone coating (Figure 18). A typical cross-section of a completely coated block is shown in Figure 19. The lighter coating in the figure is the silicone layer, the darker is the butyl rubber.

To quantify average coating thickness, all blocks were weighed and measured after preconditioning and before coating. Blocks were also weighed after each of the coatings was applied. Weights and average coating thickness data are given in Table 5. The average thickness of the butyl rubber and silicone coatings was 0.488 mm (0.019 inch) and 0.076 mm (0.003 inch) respectively.

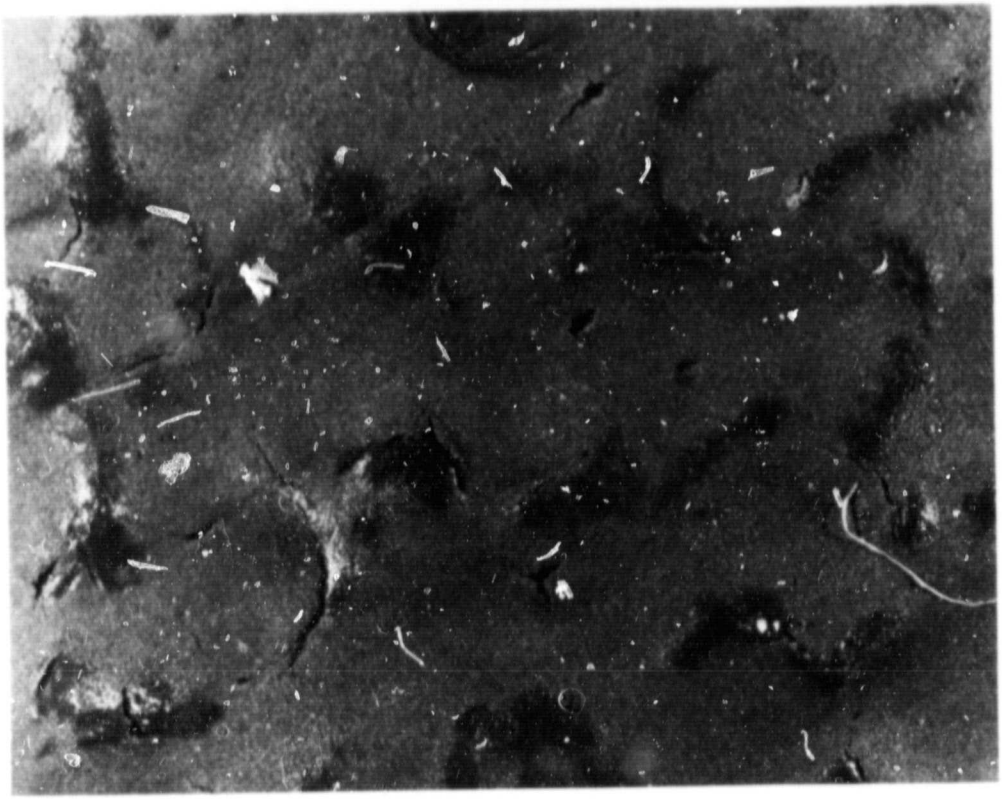

Figure 17. Cured Butyl Rubber Coating (Two Coats)

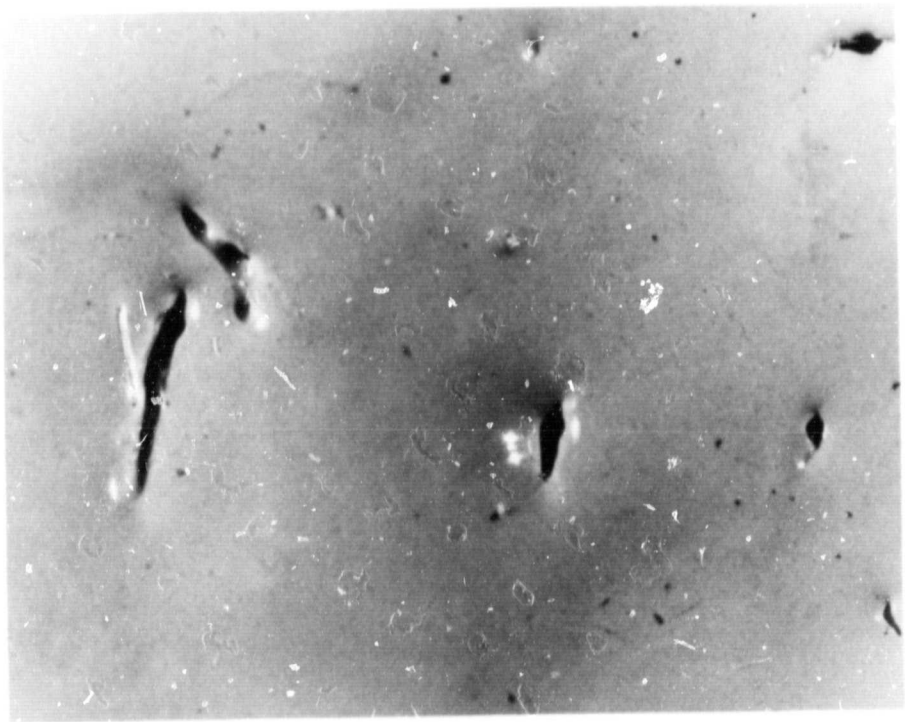

Figure 18. Cured Silicone Rubber Coating (Two Coats)

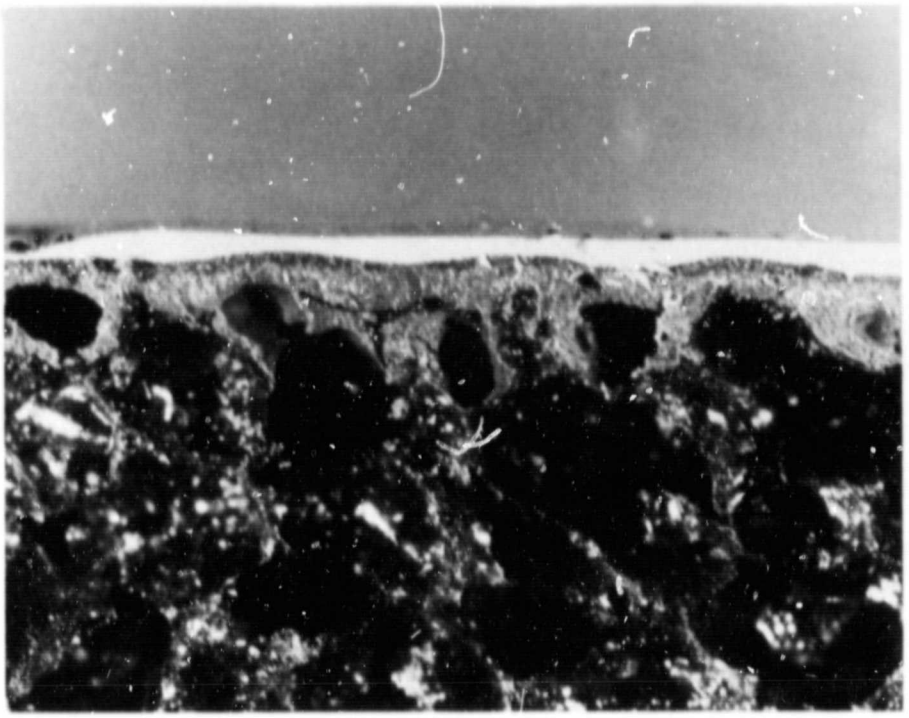

Figure 19. Cross Section, Cellular Glass Coatings

Table 5. Foamglas® Block and Coatings Initial Weights Data

I.D.	Dry Weight Grams	Block Density g/cc	Block Density (#/ft^3)	Surface Area cm^2	Surface Area (in^2)	Butyl Weight Grams	Butyl Thickness X10^{-3}m	Butyl Thickness (in.)	Silicone Weight Grams	Silicone Thickness X10^{-3}m	Silicone Thickness (in.)	Total Weight Grams
A1	835.0	0.1410	(8.80)	2352.4	(364.63)	200.4	0.483	(0.019)	30.2	0.076	(0.003)	1065.6
A2	744.4	0.1317	(8.22)	2287.7	(354.60)	217.2	0.533	(0.021)	41.6	0.102	(0.004)	1003.2
A3	813.6	0.1373	(8.57)	2349.8	(364.22)	194.2	0.457	(0.018)	28.7	0.076	(0.003)	1036.5
A4	815.9	0.1390	(8.68)	2340.3	(362.75)	222.7	0.533	(0.021)	32.0	0.076	(0.003)	1070.6
A5	808.5	0.1386	(8.65)	2334.6	(361.86)	216.2	0.508	(0.020)	14.4	0.051	(0.002)	1039.1
A6	801.2	0.1381	(8.62)	2326.3	(360.57)	220.2	0.533	(0.021)	28.6	0.076	(0.003)	1050.0
A7	806.0	0.1392	(8.69)	2324.2	(360.25)	185.5	0.457	(0.018)	26.2	0.076	(0.003)	1017.7
A8*	814.0	0.1410	(8.80)	2321.4	(359.84)	180.7	0.432	(0.017)	29.3	0.076	(0.003)	1024.0
A9*	784.7	0.1334	(8.33)	2344.1	(363.34)	197.9	0.483	(0.019)	27.8	0.076	(0.003)	1010.4
A10	759.8	0.1309	(8.17)	2326.8	(360.66)	191.7	0.457	(0.018)	29.3	0.076	(0.003)	980.8
A11	806.6	0.1384	(8.64)	2331.2	(361.34)	—	—	—	—	—	—	860.6
A12	815.2	0.1382	(8.63)	2344.8	(363.45)	—	—	—	—	—	—	815.2
A13	787.5	0.1344	(8.39)	2338.1	(362.41)	—	—	—	—	—	—	787.5
A14	760.6	0.1299	(8.11)	2338.2	(362.42)	—	—	—	—	—	—	760.6
A15	810.6	0.1379	(8.61)	2342.4	(363.07)	—	—	—	—	—	—	810.6
A16	816.1	0.1386	(8.65)	2345.6	(363.57)	—	—	—	—	—	—	816.1
A17	764.1	0.1334	(8.33)	2311.9	(358.34)	—	—	—	—	—	—	764.1
A18	785.7	0.1336	(8.34)	2342.6	(363.11)	—	—	—	—	—	—	785.7
A19*	789.1	0.1331	(8.31)	2352.6	(364.65)	—	—	—	—	—	—	789.1
A20*	782.0	0.1213	(7.57)	2464.3	(381.97)	—	—	—	—	—	—	722.0

*Control Blocks

SECTION V

FREEZE/THAW CONDITIONING

A. DISCUSSION OF THE CYCLE

The modeling of accelerated environmental exposure of materials using artificial techniques is a complex subject. The pathways by which degradation may occur range from macroscopic to molecular. The mechanism or mechanisms of initiation often differ from those of propagation. The artificial acceleration of any factor or group of factors which define the natural deterioration rate of a material may change the specific rate-determining mechanism of breakdown. Considering the synergistic effects by which chemical and physical processes often flow, unrealistic conclusions may easily be drawn with respect to natural degradation rates.

In selecting a freeze/thaw cycle for artificial aging of cellular glass, several parameters must be assumed to be potentially critical to the specific mechanism of natural freeze/thaw degradation. The temperature extremes and relative humidity during the cycle are key variables. Since cellular glass is a well-known insulator, the rate of change and dwell times of the exposure temperature are likely to be a factor. Air flow, chamber geometry and specimen location are also important. Specimen shape, support and orientation are usually design-specific and need to be defined to assure fair evaluation of the materials. If a polymer coating is being evaluated, the long-term effect of ultraviolet radiation on coating properties must be addressed.

To provide background for the freeze/thaw cycle design, such cycles used on previous cellular glass studies were carefully evaluated. Some cycles were clearly not representative of expected applications. Other cycles, those with rapid changes in exposure temperatures or short dwell times at plateau temperatures, were felt to possibly change the basic degradation mechanism. This was supported, in part, by the trend of failures found in the highly accelerated cycles.

The cycle used by Argoud in 1978 (see Figure 6) seemed to be fairly representative of the typical environment expected. However, to allow the water vapor and pooled water to experience the influence of a high driving force into the Foamglas®,[23] one of the high temperature plateaus was replaced with a low temperature dwell just above freezing. It was also determined that the humidity was maintained at an unrealistically high level, so the humidity was stabilized at 85% RH at 30°C and the chamber temperature was used to establish the humidity levels at temperatures other than 30°C. With these changes, a freeze/thaw cycle quite similar to that found in nature was established.

The final cycle which was decided upon is shown in Figure 20.

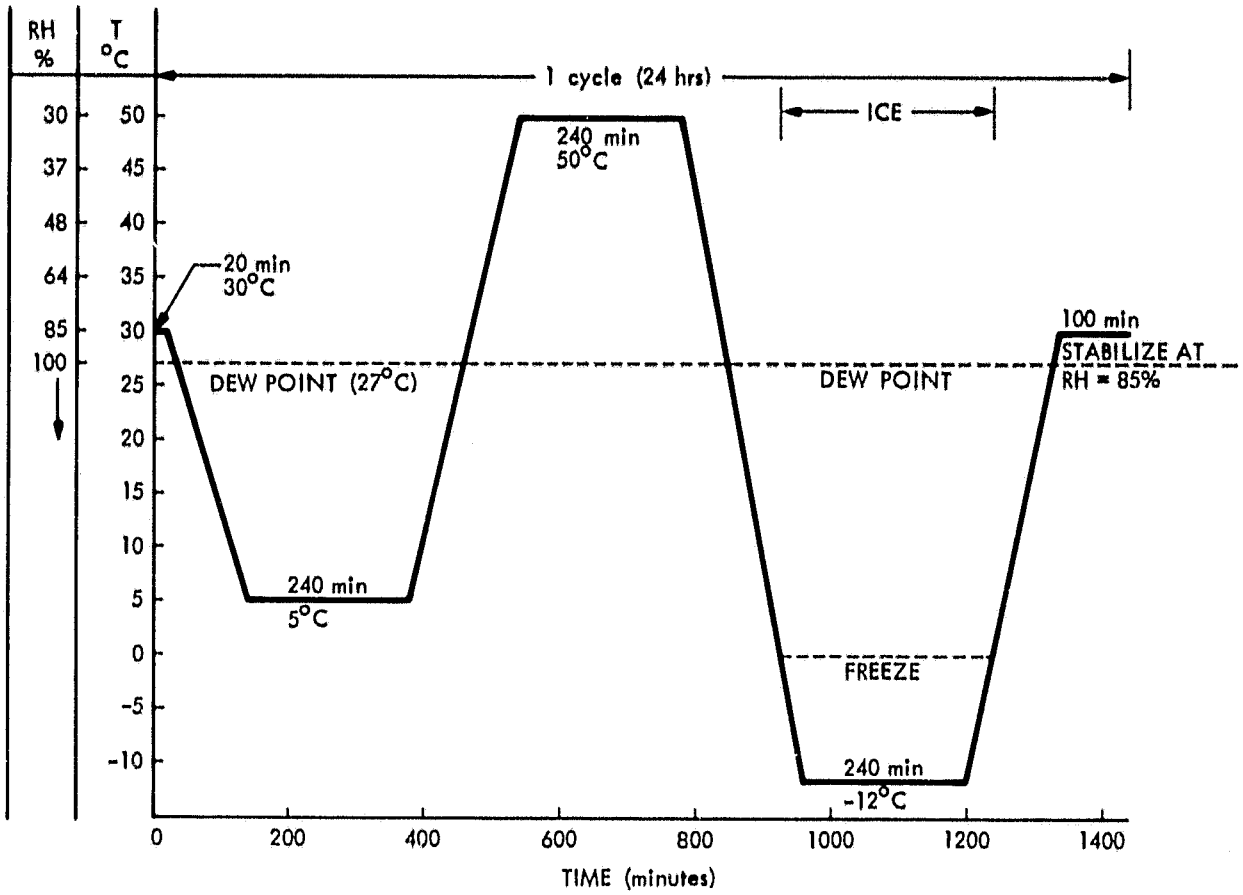

Figure 20. Freeze/Thaw Cycle, Cellular Glass (-12° to +50°C)

B. FACILITIES

The cellular glass blocks were environmentally conditioned in a 27-cubic-foot Conrad model FD-30-5-5 environmental chamber controlled by a Thermotron Microcomputer Programmer model 013025. This system allowed straightforward computer control of the temperature and humidity in the chamber. Wet and dry bulb temperatures were monitored throughout the test using the chamber's recording charts and various digital data loggers (See Figure 21).

C. CHAMBER CHARACTERIZATION

Before conditioning the actual test blocks, a chamber characterization and cycle evaluation run was done. The chamber was loaded as shown in Figure 22 with several 2- by 5- by 18-inch blocks, plus four thicker Foamglas® blocks, instrumented with thermocouples. The thermocoupled blocks had sensors on both the top and bottom surfaces. There was one thermocoupled block and one airstream thermocouple on each of the four shelves of the chamber. As the airflow in the chamber is from the bottom to the top, six of the 2-inch-thick blocks were placed on the lowest shelf to disrupt and randomize airflow. A

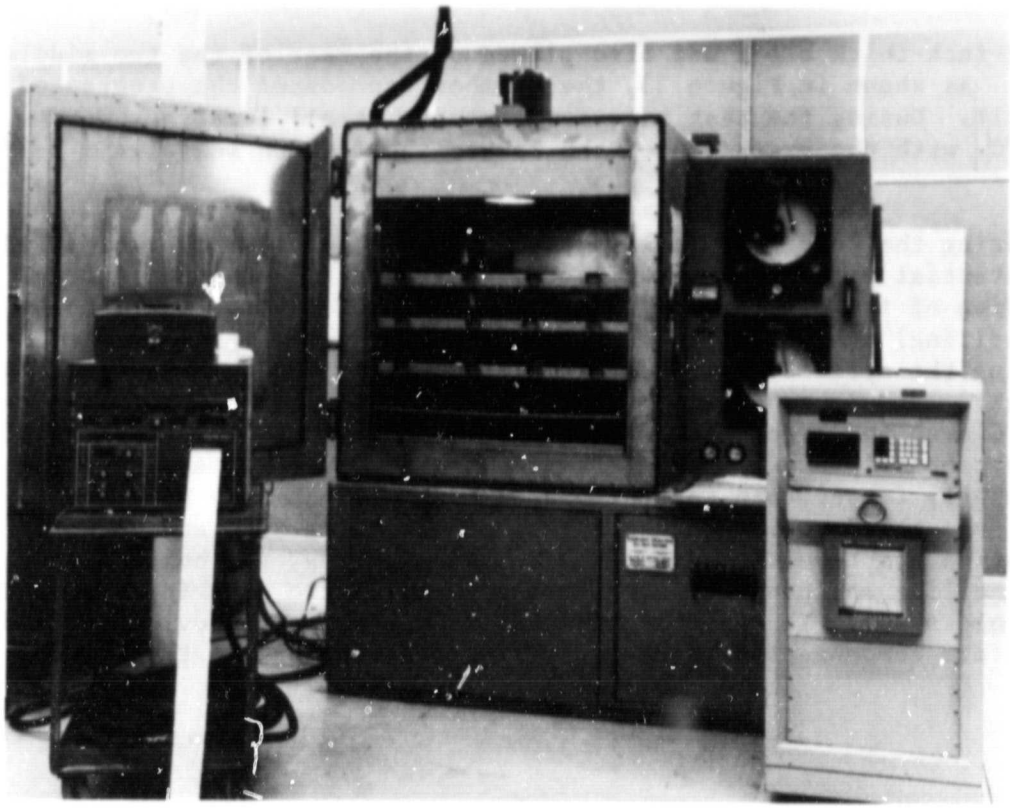

Figure 21. Environmental Control Chamber, Control Unit and Data Logger

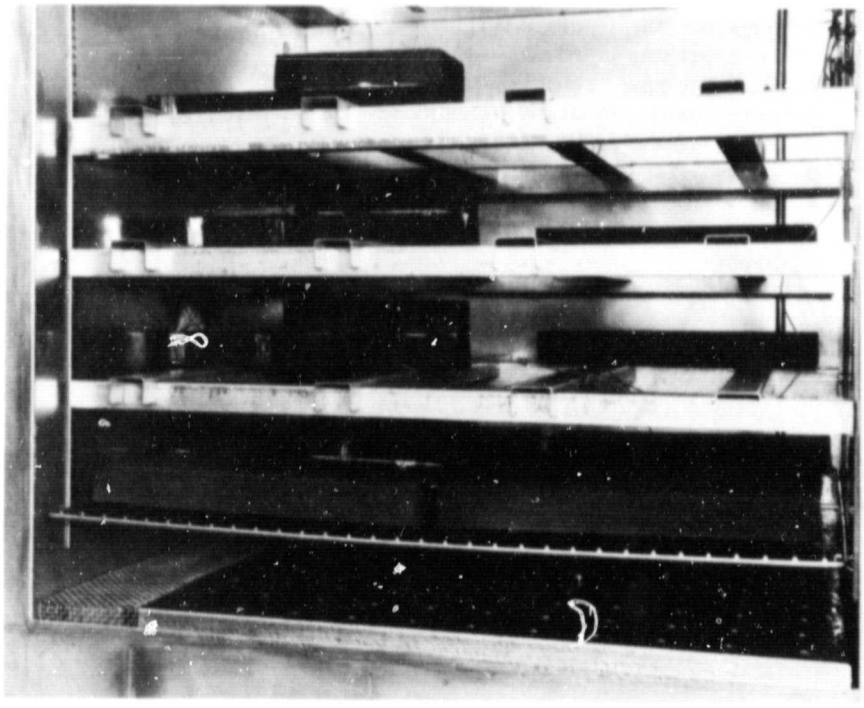

Figure 22. Foamglas® in Chamber Characterization Run

single 2-inch-thick block was also placed on the rear of the two middle shelves. As shown in Figure 23, the chamber reproduced the programmed cycle quite well. During the test run, temperatures at all locations were within about 2°C, with the exception of the lowest shelf which was always 2-3°C higher.

During the test run, it was observed that the upper thermocoupled block had substantial water pooling while the other blocks did not. Careful examination of the chamber led to the discovery of several small holes in the upper (ceiling) condenser pan. This would allow water which condensed on the pan during the cycle to drip from the left side of the ceiling directly onto the block. This is especially significant in that this was the same chamber used by Giovan and Argoud (see Figure 11) in which most uncoated cellular glass specimens (placed on the left side of the chamber) were shown to degrade significantly faster than coated (placed on the right side of the chamber). To eliminate this problem in the actual conditioning run, and to ensure random condensation and resultant dripping from the ceiling, the holes were plugged and the ceiling was covered with stainless steel wire mesh (approximately 1-inch hole size). It was observed that this technique provided considerably more uniform condensation while minimizing restrictions to the chamber airflow.

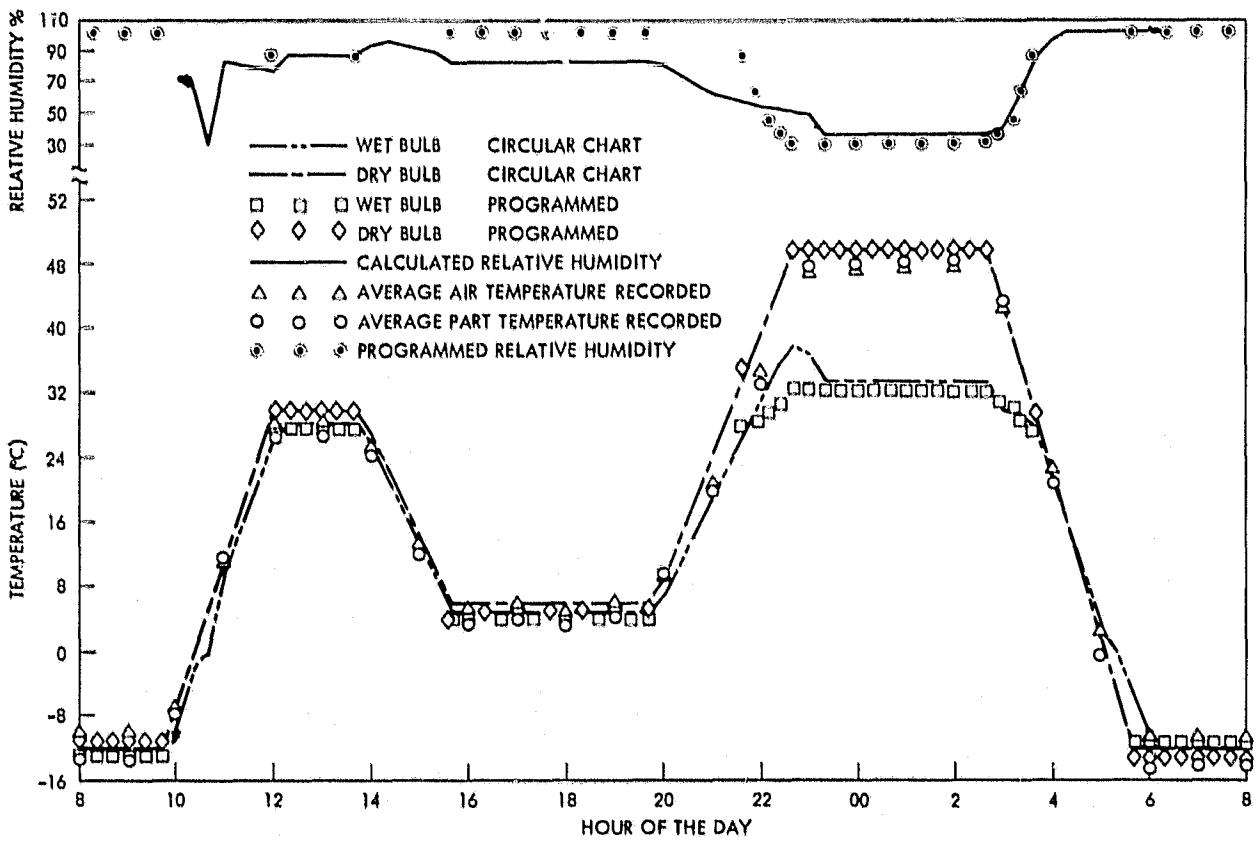

Figure 23. Humidity Chamber Test Cycle, Oct. 5 and 6, 1980

Table 6 shows the temperature spread of the thermocoupled blocks with respect to air temperature within the chamber. Typical thermal lag of the Foamglas® glass blocks was approximately 20 minutes.

D. SPECIMEN CONDITIONING AND SAMPLING PLAN

Figure 24 shows the coated and uncoated Foamglas® blocks in position in the chamber before conditioning. Note that at the time of the photograph, the stainless steel mesh had not yet been added. It was added, however, before the start of the experimental program.

The samples were arranged such that the shelf location directly over and under any given block was vacant. This allowed improved air circulation and provided for more random "weathering." There were four blocks to a shelf, two coated and two uncoated.

Figure 25 shows the method which was used for sampling the conditioned blocks and the location of the 4- by 5- by 18-inch dummy block for thermocouples. R1, R2, L1 and L2 from the upper shelves were sampled at only seven cycles, since if significant degradation was going to happen immediately it should be easily observable. The samples from the upper shelves (R1, R2, L1 and L2) allowed a midpoint in the data. The final group: R3, R4, L3 and L4 from both the top and the bottom provided a third datapoint and allowed insight to specific variation in conditioning rates caused by block location with respect to height within the chamber.

E. OBSERVATIONS

On several occasions during the period of freeze/thaw conditioning, the chamber was opened and visual observations were made. The chamber was only opened during the room-temperature portion of the cycle. On every occasion all Foamglas® blocks were noted to be wet on all sides. No pooled water was noted; however individual condensed water droplets of approximately 0.125-inch-diameter were typically visible on coated blocks. Also, droplets of water were noted to be condensing randomly on the stainless steel wire mesh suspended from the ceiling.

Very little change of appearance was noted between unconditioned and fully conditioned blocks. All uncoated blocks appeared wetter near the center of the faces and somewhat drier near the edges and corners. The later (38-, 52- and 53-cycle) coated blocks were observed to be slightly adhered to the chamber racks. This was apparently due to cold flow of the polymer coatings as evidenced by flattening and local thinning of the silicone overcoat which resulted in slight darkening as the butyl rubber coating became more exposed. In one instance the adhesion to the racks was great enough to cause the coatings to tear away the upper layer of glass cells. This was very localized and outside the highly stressed area of the tested specimen and therefore thought not to effect the mechanical test results. No significant spalling of uncoated Foamglas® specimens was observed at the end of the freeze/thaw conditioning phase.

Table 6. Typical Block Temperatures* During Conditioning

Hour	Air (Avg.)	Block (Avg.)	Block (Low)	Block (High)
00	23.8	33.6	28.9	35.9
01	3.3	13.8	8.1	16.4
02	-11.7	-5.8	-9.8	-3.8
03	-11.6	-10.8	-12.0	-10.3
04	-12.1	-11.3	-12.1	-10.9
05	-11.6	-11.3	-12.2	-11.1
06	-7.8	-10.6	-11.3	-9.5
07	10.0	3.5	1.8	6.8
08	27.2	20.2	18.4	23.2
09	29.0	28.1	27.9	28.5
10	26.2	28.3	27.4	28.8
11	14.0	19.3	16.2	20.7
12	6.0	8.7	6.3	9.8
13	5.7	6.2	5.3	6.5
14	5.8	5.9	5.7	6.1
15	5.6	6.0	5.3	6.2
16	8.7	6.6	6.1	7.5
17	20.0	15.5	14.4	17.5
18	32.4	27.1	25.8	29.3
19	47.2	42.6	39.9	46.3
20	46.9	47.2	44.4	48.8
21	47.2	48.0	45.9	49.0
22	47.1	48.2	46.4	49.0
23	43.4	47.5	46.7	48.6
24	22.3	33.0	28.6	35.3

*Note: All temperatures given in ^{o}C.

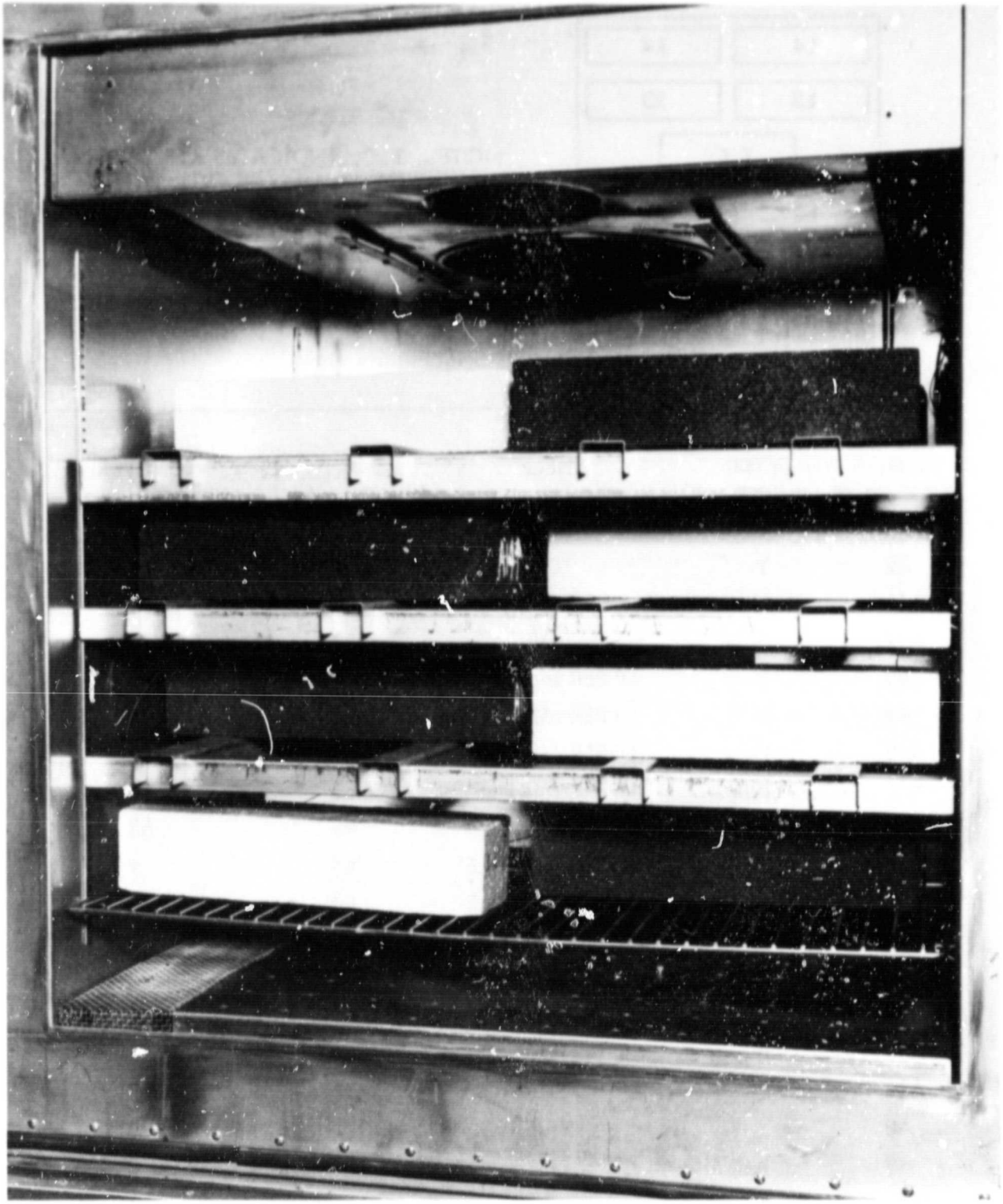

Figure 24. Foamglas® Blocks Prior to Freeze/Thaw Conditioning

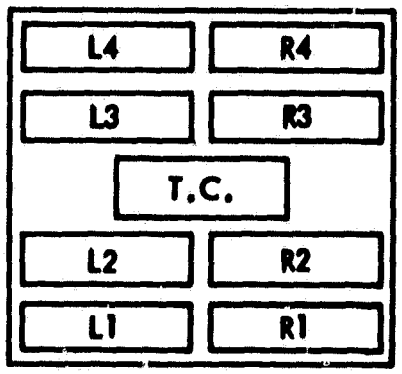

NOTE: T.C. INDICATES LOCATION OF DUMMY BLOCK WITH BURIED THERMOCOUPLES (ALL EXCEPT BOTTOM SHELF)

TYPICAL CHAMBER SHELF (plan view)

BLOCK I.D.	COATED (Y/N)	SHELF	LOCATION	DURATION (CYCLES)
A1	Y	TOP	L4	52
A2	Y	TOP	L2	38
A11	N	TOP	R3	52
A12	N	TOP	R1	38
A3	Y	UPPER MIDDLE	R4	52
A4	Y	UPPER MIDDLE	R2	38
A13	N	UPPER MIDDLE	L3	52
A14	N	UPPER MIDDLE	L1	38
A5	Y	LOWER MIDDLE	R3	53
A6	Y	LOWER MIDDLE	R1	7
A15	N	LOWER MIDDLE	L4	53
A16	N	LOWER MIDDLE	L2	7
A7	Y	BOTTOM	L3	53
A10	Y	BOTTOM	L1	7
A17	N	BOTTOM	R4	53
A18	N	BOTTOM	R2	7
A8	Y	--	CONTROL	0
A9	Y	--	CONTROL	0
A19	N	--	CONTROL	0
A20	N	--	CONTROL	0

Figure 25. Cellular Glass Freeze/Thaw Cycling Location and Sampling Plan

SECTION VI

MECHANICAL TESTING

A. MODULUS OF RUPTURE OR BEAM PREPARATION

After the cellular glass blocks had undergone environmental conditioning and had been checked for gross weight changes, they were cut into eight four-point bend specimens and labelled (see Figure 26). The cutting was done in a manner to produce eight specimens of approximately equal thickness and width. The cutting was done with a diamond grit band saw blade. Labelling was consistent in that specimens A and E were always from the surface which was uppermost during environmental conditioning.

B. METHOD AND FACILITIES

The modulus of rupture (MOR) and modulus of elasticity in bending were determined using the four-point bend technique shown in Figures 27 and 28. The test fixtures and methods which were used had been developed for an earlier cellular glass evaluation program.[1] The specimens were always loaded with their outermost face in tension, to allow measurement of the maximum effect of any freeze-thaw degradation by subjecting the most weathered surfaces (those closest to the environment) to the highest strain conditions. This means the top of blocks A, B, E, and F, and the bottom of blocks C, D, G and H, were loaded in tension. All coatings were left on the samples for the

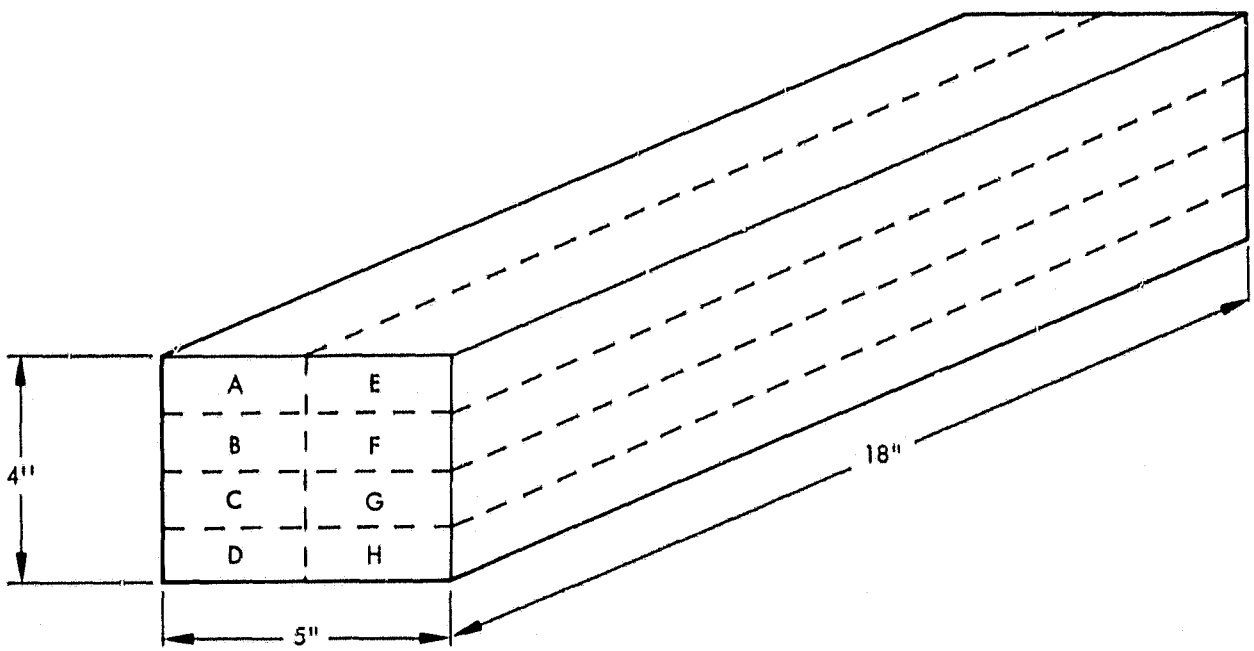

Figure 26. Four-Point Bend Specimen Cutting Schedule

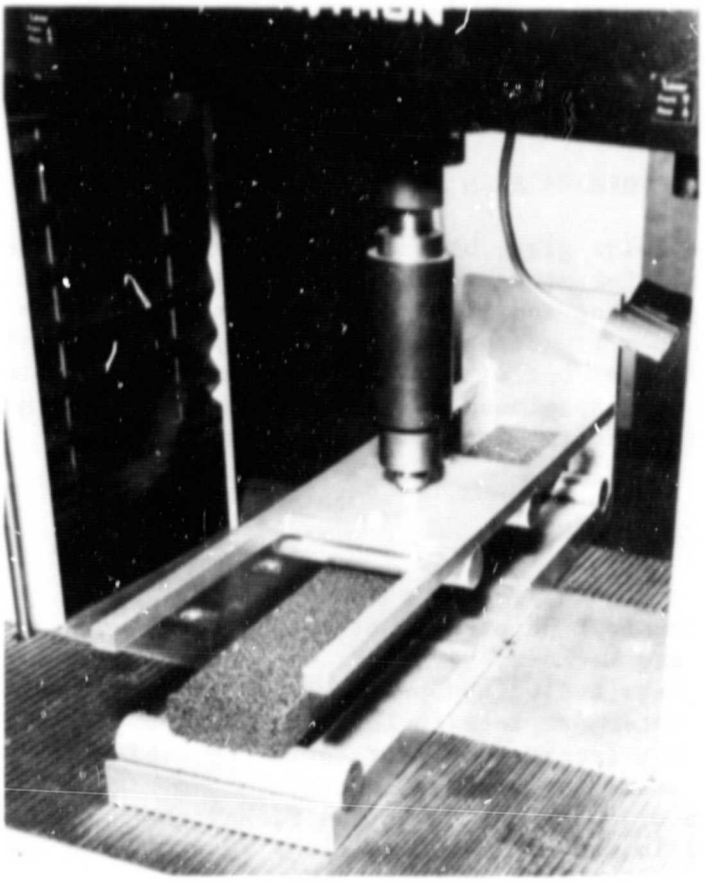

Figure 27. Four-Point Bend Test Fixture

test. The typical loading rate used during testing was 0.2 in/min, and time-to-failure in the test was typically 9 to 12 seconds. An Instron Universal testing machine Model 1122 and an Instron Microcon I data recorder (see Figure 29) were used for all tests.

C. APPROACH

Since testing included coated and uncoated Foamglas® specimens, the effect which the coatings had on the computed mechanical properties was evaluated. Figure 30 shows Case I, an uncoated Foamglas® specimen.

For Case I:

$$\Sigma EI = E \frac{t^3 b}{12} \qquad (6\text{-}1)$$

by setting

t = 1.0" (specimen thickness)
b = 2.5" (specimen width)
E = 208 x 10^3 psi (Foamglas® modulus)

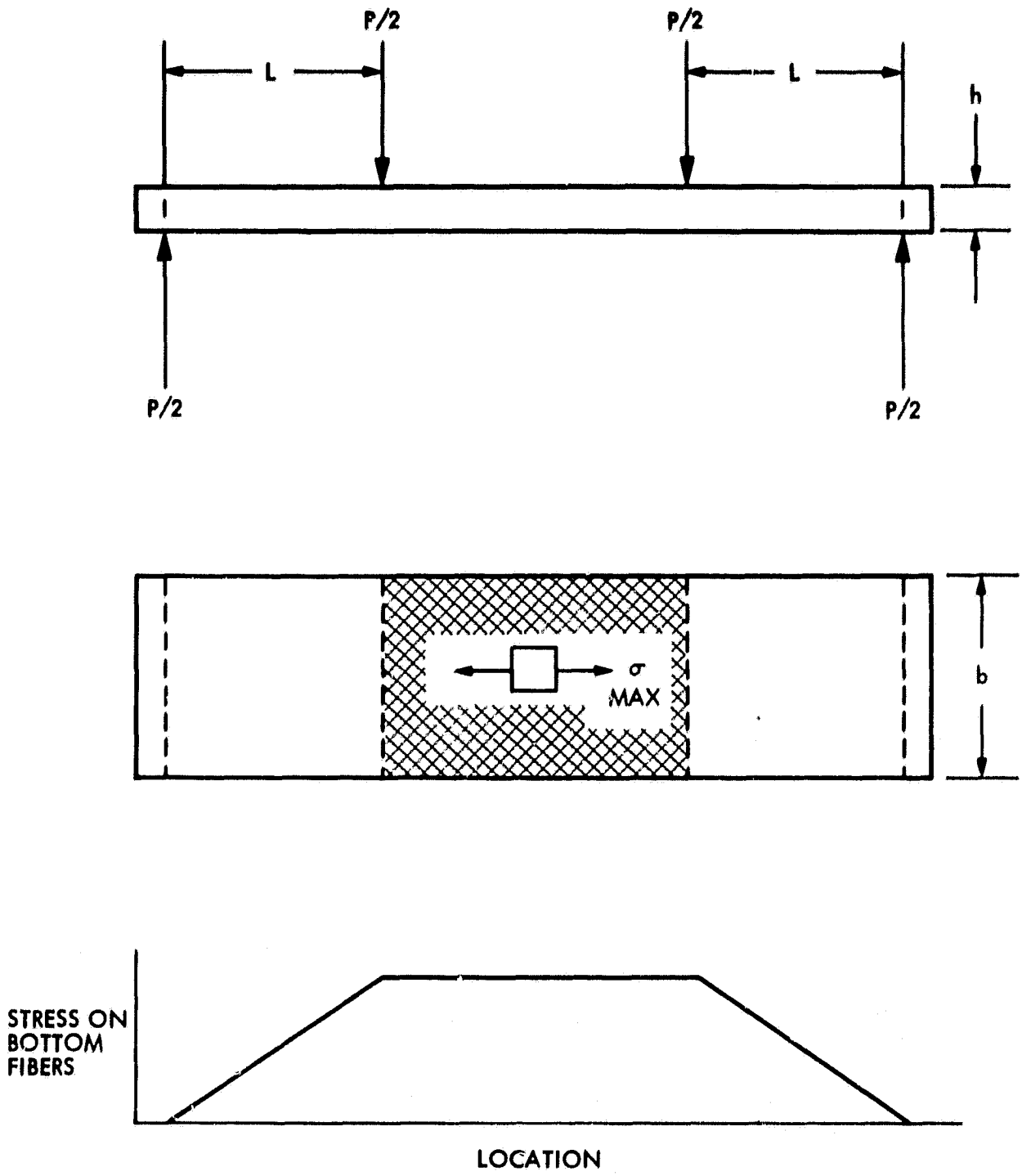

Figure 28. Four-Point Bend Test Configuration

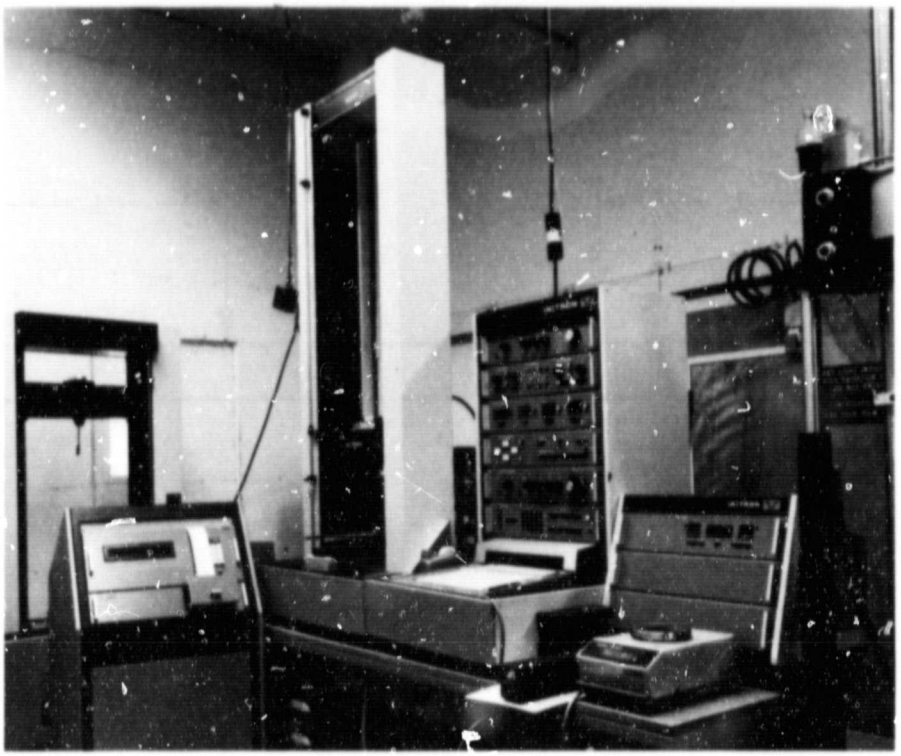

Figure 29. Testing Machine and Data Logger

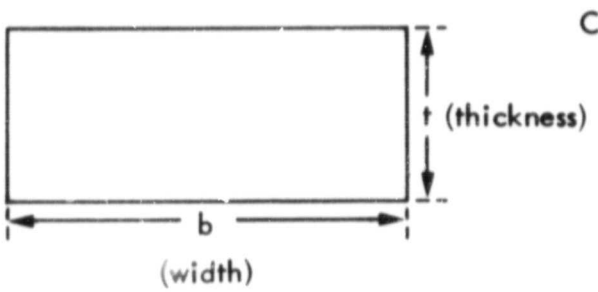

Figure 30. Case I, Uncoated Foamglas® Specimen

$$\Sigma EI = 43.33 \times 10^3 \text{ lb-in}^2 \qquad (6\text{-}2)$$

the stress (σ) in the outermost tensioned cellular glass surface is:

$$\sigma = \frac{McE}{\Sigma EI} \qquad (6\text{-}3)$$

by setting

$$c = \frac{t}{2} = 0.5"$$

$$M = 4PL = 40 \text{ in-lb}$$

$$\sigma = 96.0 \text{ psi} \qquad (6.4)$$

Figure 31 shows Case II specimens, those which had only a side coating (specimens B, C, F and G).

Assuming no twisting occurred during the test:

$$\Sigma EI = E_1 \frac{t^3 b_1}{12} + E_2 \frac{t^3 b_2}{12} + E_3 \frac{t^3 b_3}{12} \qquad (6\text{-}5)$$

By setting:

$b_1 = 2.478"$
$b_2 = 0.019"$
$b_3 = 0.003"$
$t = 1.0"$
$E_1 = 208 \times 10^3$ psi (cellular glass)
$E_2 = 10 \times 10^3$ psi (butyl coating)
$E_3 = 10 \times 10^3$ psi (silicone coating)

(the values for E_2 and E_3 are estimated "worst case" values)

$$\Sigma EI = 42.97 \times 10^3 \text{ lb-in}^2 \qquad (6\text{-}6)$$

The stress in the outermost tensioned surface of the specimen is:

$$\sigma = \frac{McE_1}{EI} \qquad (6\text{-}7)$$

by setting

$$c = \frac{t}{2} = 0.5"$$

$$M = 4PL = 40 \text{ in-lb}$$

$$\sigma = 96.8 \text{ psi} \qquad (6\text{-}8)$$

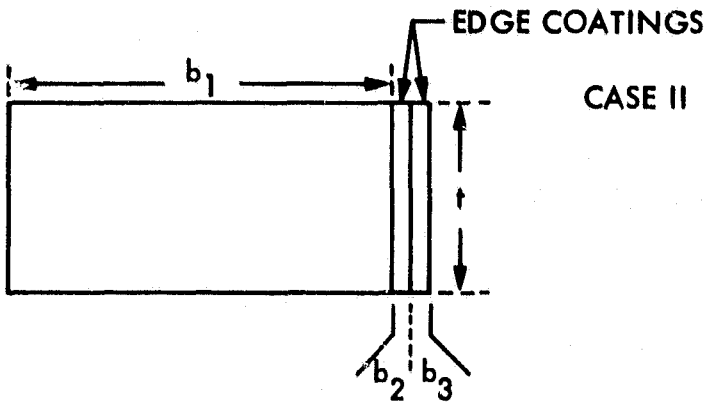

Figure 31. Case II, Side-Coated Specimens

Since equation (6-4) and (6-8) differ by less than 1%, we may say the stiffening effect of the edge coatings on the mechanical properties of specimens B, C, F and G is negligible.

Based on this information, the properties calculated for all coated specimens (B, C, F and G) assumed the full dimensions of the specimens to be entirely cellular glass.

The Case III specimens (A, D, E and H) have both edge and tensioned face coatings, as shown in Figure 32. The effect of the edge coating was again assumed negligible and the effect of the face coating was evaluated.

For Case III, x is the shift in the position of the neutral axis of the composite beam due to the structural effect of the coatings on the tensioned face.

$$\bar{x} = \frac{bt_2E_2\left(\frac{t_1 + t_2}{2}\right) + bt_3E_3\left(\frac{t_1 + 2t_2 + t_3}{2}\right)}{t_1bE_1 + t_2bE_2 + t_3bE_3} \qquad (6\text{-}9)$$

by setting

$t_1 = 0.978"$
$t_2 = 0.019"$
$t_3 = 0.003"$
$b = 2.5"$
$E_1 = 208 \times 10^3$ psi (cellular glass)
$E_2 = 10 \times 10^3$ psi (butyl coating)
$E_3 = 10 \times 10^3$ psi (silicone coating)

These estimated values for E_2 and E_3 are "worst case" approximations (higher than average modulus).

$$\bar{x} \cong 0.001" \qquad (6\text{-}10)$$

$$\Sigma EI = \sum_{i=1}^{3} E_i \frac{bt_i^3}{12} + (\bar{x})^2 bt_1E_1 + \left(\frac{t_1 + t_2}{2} - \bar{x}\right)^2 bt_2E_2 + \left(\frac{t_1 + 2t_2 + t_3}{2} - \bar{x}\right)^2 bt_3E_3 \qquad (6\text{-}11)$$

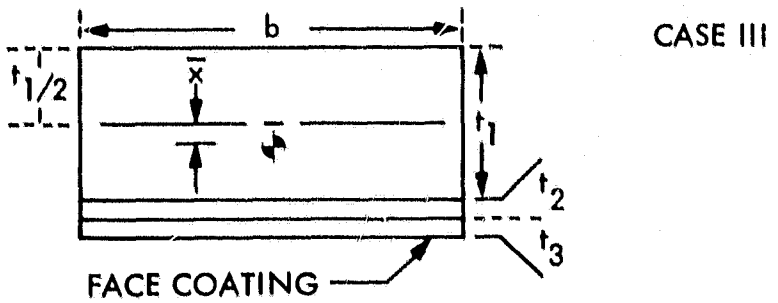

Figure 32. Case III, Edge- and Face-Coated Specimens

$$= \frac{b}{12}\left(E_1 t_1^3 + E_2 t_2^3 + E_3 t_3^3\right) + b\left[(\bar{x})^2 t_1 E_1 + \left(\frac{t_1 + t_2}{2} - \bar{x}\right)^2 t_2 E_2 + \left(\frac{t_1 + 2t_2 + t_3}{2} - \bar{x}\right)^2 t_3 E_3\right] \quad (6\text{-}12)$$

$$\Sigma EI = 40.67 \times 10^3 \text{ lb-in}^2 \quad (6\text{-}13)$$

The stress in the outermost tensioned cellular glass surface is:

$$\sigma = \frac{McE_1}{\Sigma EI} \quad (6\text{-}14)$$

By setting

$$c = \frac{t_1}{2} - \bar{x} = 0.488 \text{ in.}$$

$$M = 4PL = 40 \text{ in-lb}$$

$$\sigma = 99.83 \text{ psi} \quad (6\text{-}15)$$

This differs from Case I by nearly 4%; therefore the effect of the coatings on the tensioned surface is significant. To simplify the calculation of stress in Case III, a modified Case I approximation was used. The approximation used in the Case I equations with t = 0.978 and b = 2.5 (disallowing the thicknesses of the coatings on the tensioned face):

$$EI = 40.54 \times 10^3 \text{ lb-in}^2 \quad (6\text{-}16)$$

$$\sigma = 100.36 \times 10^3 \text{ psi} \quad (6\text{-}17)$$

This approximation differs from that calculated in 6-15 by less than 1% and was therefore used in the calculation of the mechanical properties of all coated specimens, A, D, E and H.

It is known that the mechanical response of polymers is highly sensitive to strain rates, and, as a significant change in the values of E_2 and E_3 might compromise the applicability of the Case III approximation, the strain rate developed in the conformal coatings during the test was evaluated. The maximum strain rate experienced was found to be less than 0.4 in/min. This is significantly below the level at which strain rate would have an appreciable effect upon the assumed modulus for these materials.[24]

D. PROCEDURE

The width and thickness values used in the calculations were averages of two and four measurements, respectively. For all calculations the weight of the test fixture was added to the induced load. The fixture weight was 1176.5 gm (2.594 lb) for the seven-cycle test. All other tests used a 942.5 gm (2.078 lb)

fixture. Internal machine and fixture deflections were accommodated using the following experimentally determined equation:

$$D_1 = D_o - \frac{L - 0.79}{12598} \qquad (6\text{-}18)$$

where D_o was the measured deflection (in inches) and L was the applied load (in pounds).

The modulus of rupture (MOR) was calculated using the following equation:

$$\text{MOR (psi)} = \frac{19.5P}{wt^2} \qquad (6\text{-}19)$$

where:

P is the total load in pounds
w is the average width in inches
t is the average thickness in inches
and 19.5 is a test geometry constant expressed in inches.

Young's modulus (E) was calculated using the following equation:

$$E = \frac{1065.25P}{D_1 wt^3} \qquad (6\text{-}20)$$

where P, D_1, w, and t are as previously defined and 1065.25 is a test geometry constant expressed as in^2.

SECTION VII

DISCUSSION OF RESULTS

A. WEIGHT CHANGES DURING CONDITIONING

All Foamglas® blocks were weighed before and after conditioning and the percent weight change calculated. These results are shown in Table 7.

Table 7. Foamglas® Weight Change Before and After Conditioning

Block	Coated	Cycles	Initial Weight (g)	Final Weight (g)	% Weight Change
A8	X	0	1024.0	1022.1	-0.19
A9	X	0	1010.4	1007.8	-0.26
A19		0	789.1	789.1	-0.25
A20		0	782.0	780.1	-0.24
A6	X	7	1050.0	1047.7	-0.22
A10	X	7	980.8	977.9	-0.30
A16		7	816.1	815.5	-0.07
A18		7	785.7	785.9	+0.03
A2	X	38	1003.2	998.3	-0.49
A4	X	38	1070.6	1065.5	-0.48
A12		38	815.2	812.9	-0.28
A14		38	760.6	761.0	+0.05
A1	X	52	1065.6	1060.7	-0.46
A3	X	52	1036.5	1031.9	-0.44
A11		52	806.6	806.5	-0.01
A13		52	787.5	787.1	-0.05
A5	X	53	1039.1	1035.7	-0.33
A7	X	53	1017.7	1013.3	-0.43
A15		53	810.6	810.2	-0.05
A17		53	764.1	763.1	-0.13

The weight changes generally were very low for uncoated Foamglas®. Coated Foamglas® showed a gradual weight loss with increasing conditioning time. For all samples the weight change was less than 0.5% and may be considered insignificant. The higher weight loss in the coated specimens probably indicates a slow evolution of volatiles from the coating system.

B. OBSERVATIONS

No obvious cracking, spalling or leaching of coated or uncoated Foamglas® was observed after 53 freeze/thaw cycles. Figures 33 and 34 illustrate cross-sections of the upper surfaces of typical uncoated Foamglas specimens after 0 and 53 cycles, respectively. Figures 35 and 36 are top views of the same specimens. The specimens were virtually indistinguishable.

C. DENSITY CHARACTERISTICS OF TEST SPECIMENS

Density for uncoated Foamglas® specimens was determined to assist in evaluating the variability which might be induced by significant material fluctuations. Eighty specimens were evaluated and a histogram of the results is shown in Figure 37. The densities were quite confined, ranging between 7.57 and 9.08 $lbs/in.^3$. With a range of only 1.51 $lbs/in.^3$, this sample may be considered to be reasonably representative of a single density population (i.e., not multimodal).

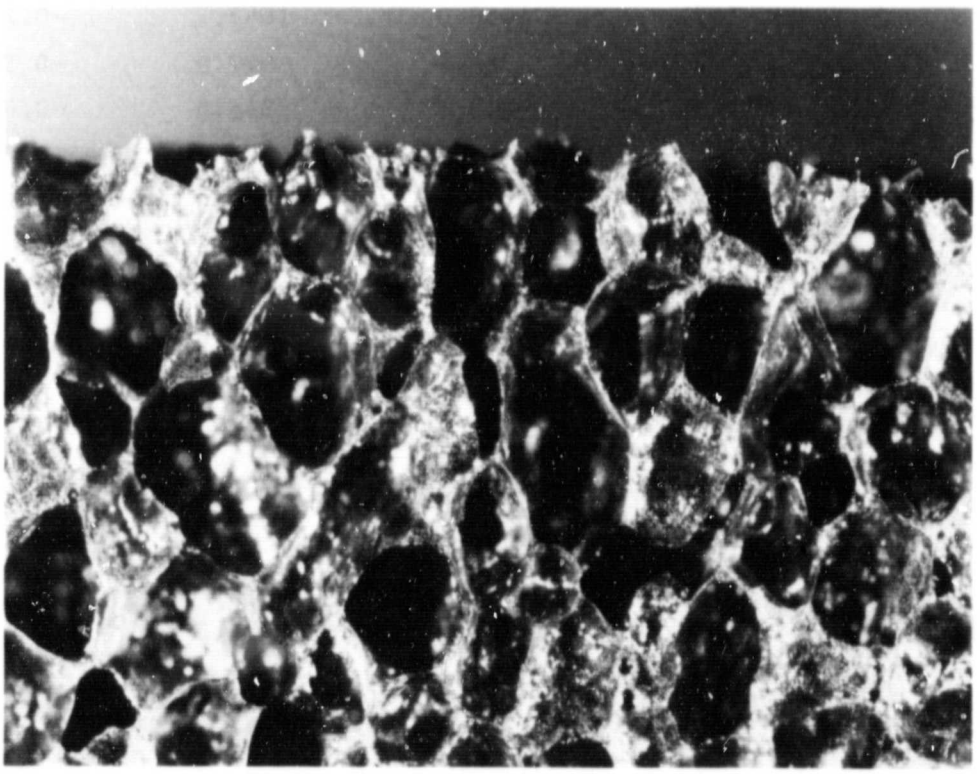

Figure 33. Foamglas® Control, Cross Section (0 Cycles)

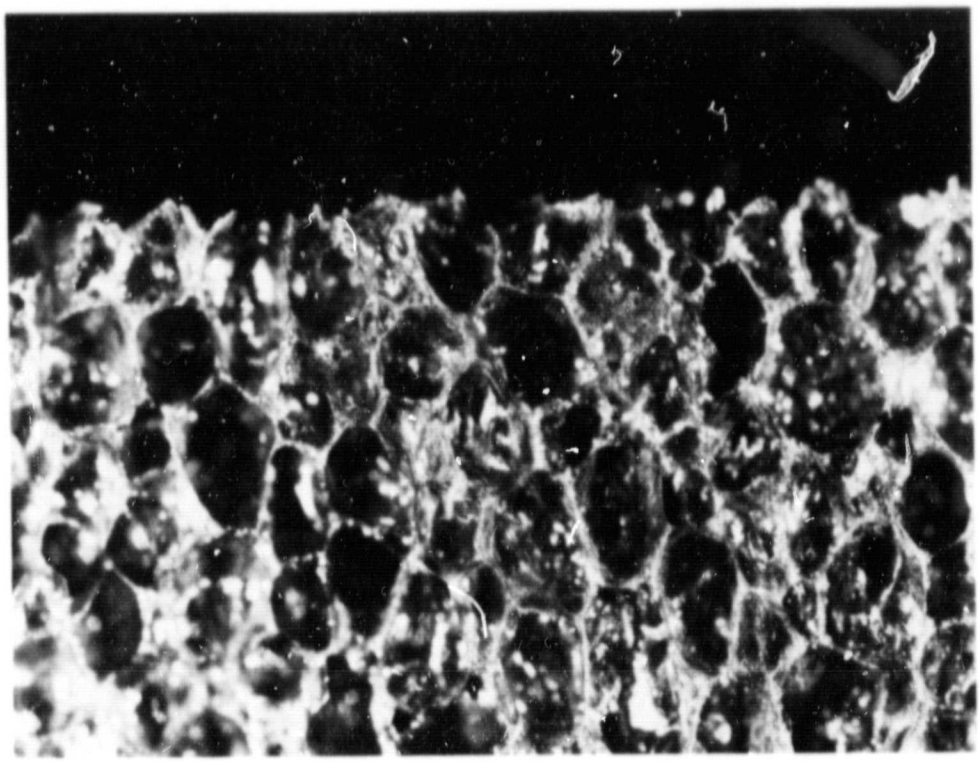

Figure 34. Foamglas® Conditioned, Cross Section (53 Cycles)

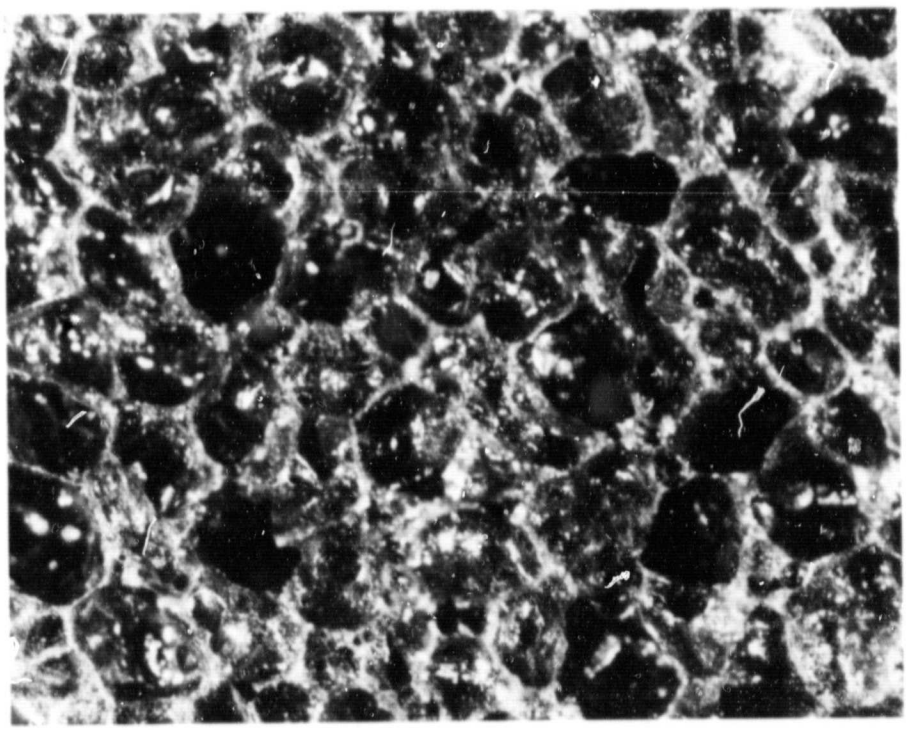

Figure 35. Foamglas® Control, Top View (0 Cycles)

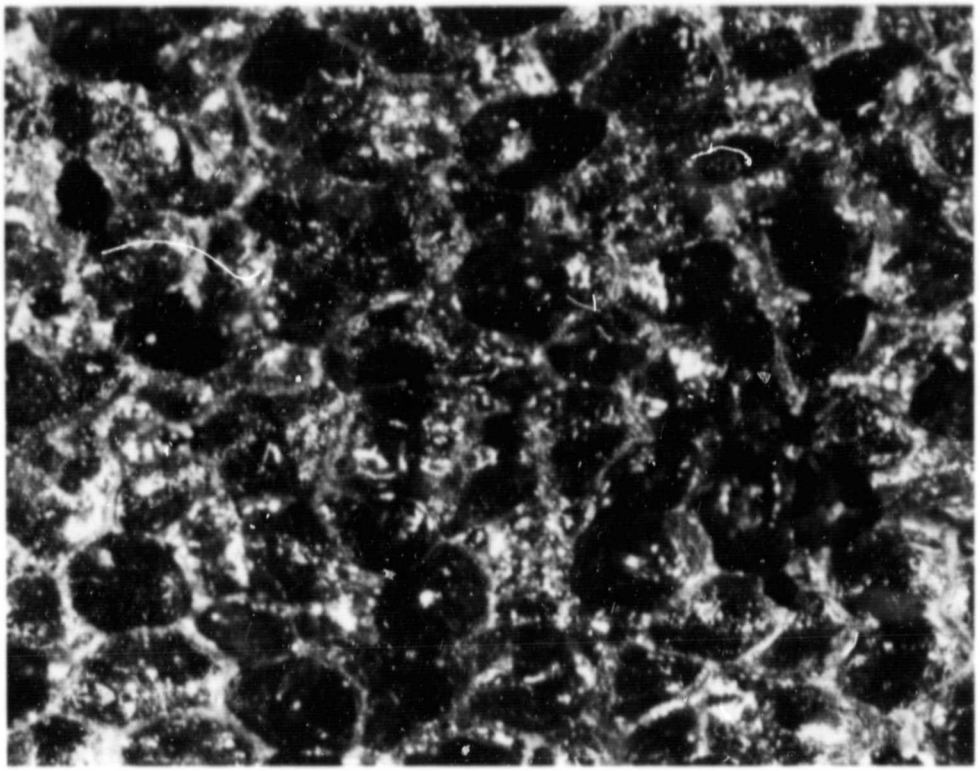

Figure 36. Foamglas® Conditioned, Top View (53 Cycles)

D. MECHANICAL TEST RESULTS

The values found in the following discussions of mechanical test results are calculated from the raw test data found in Appendix A.

The classical statistical analysis methodology, from which the following tables and figures were developed, employed the following formulas:[25]

$$\text{MEAN}(\bar{x}) = \frac{\Sigma x}{N} \qquad (7\text{-}1)$$

where N = size of sample group A
X = sample parameter value

$$\text{Standard deviation} = \sigma = \sqrt{\frac{\Sigma(x - \bar{x})^2}{N-1}} \qquad (7\text{-}2)$$

$$\text{Variance} = \sigma^2 \qquad (7\text{-}3)$$

$$\text{Coefficient of Variation} = \text{C.V.} = \sigma/\bar{x} \qquad (7\text{-}4)$$

Since the sample groups were small, the N-1 (unbiased) weighting was used for the calculation of σ.

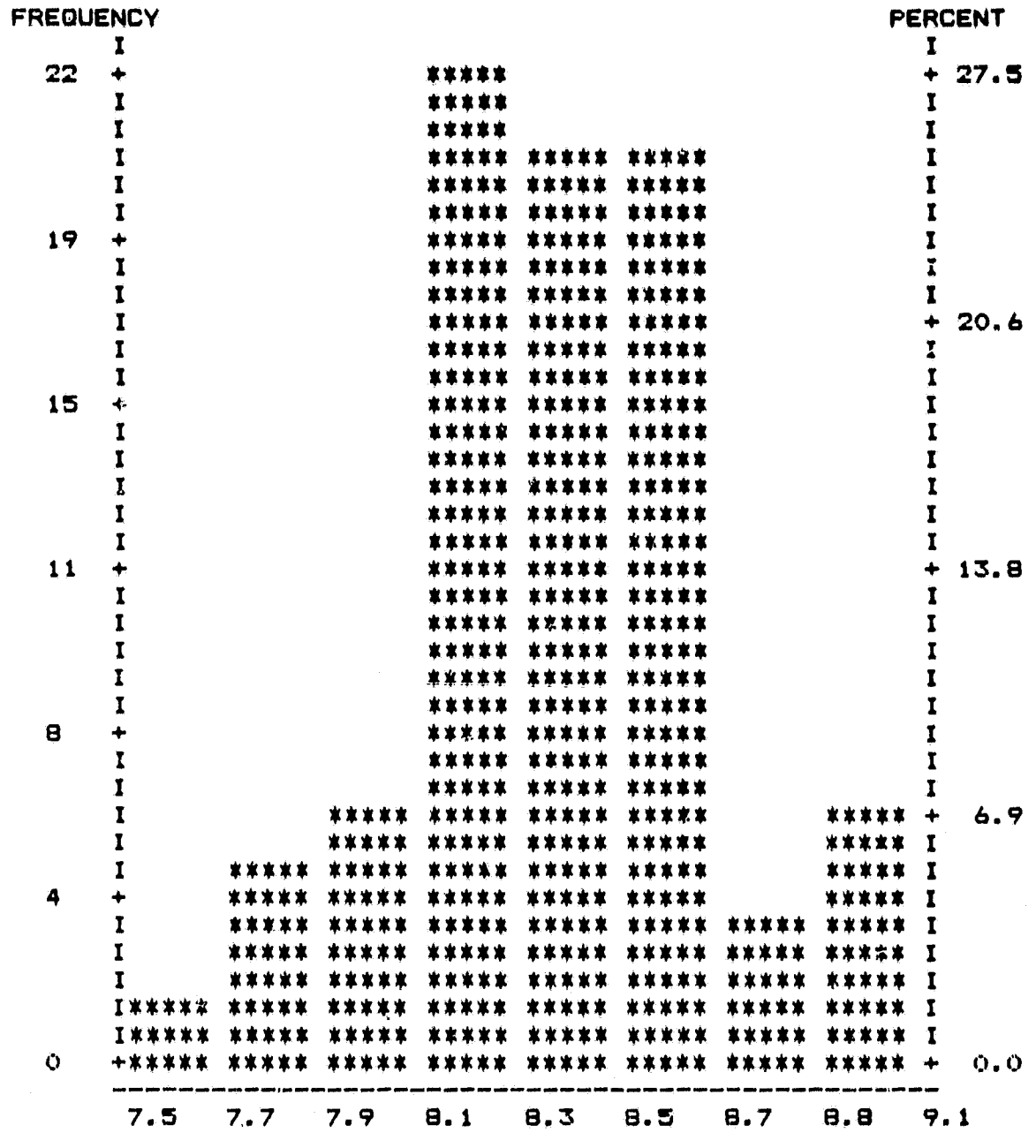

Descriptive Statistics

Mean:	8.4 lbs/ft.^{3}	Skewness:	-0.29 -0.29
Variance:	0.081	Kurtosis:	0.445 0.455
Standard Deviation:	0.284	Coeff. of Variation:	0.03

Figure 37. Density of Foamglas®

1. Modulus of Rupture (MOR)

The environmental conditioning was expected to affect the test specimens differently with respect to origin within parent blocks. Specifically, specimens A and E (top) were expected to experience the most severe environments, and as such were treated as a distinct group. Specimens D and H (bottom) were also expected to experience a harsh environment, and were therefore treated as a separate group. Specimens B, C, F and G (middle) were expected to be less affected by conditioning and were also considered as a separate group.

Table 8 displays the statistics for the top, middle and bottom groups of coated and uncoated Foamglas MOR specimens with respect to conditioning cycle number. Inspection of the data in this table did not reveal a clear trend of degradation as a function of cycle number. There was also no obvious pattern to the difference in materials properties as a function of origin within the parent block (e.g., group A, E versus group B, C, F, G). Since the freeze/thaw conditioning apparently had no clear effect upon the materials properties, it was assumed that the effect of degradation was so slight as to be indistinguishable from the inherent variability of the basic, unexposed material. This assumption was statistically tested for significance using the Chi-squared (X^2) and one-way analysis of variance (ANOVA) tests for the variances and means, respectively.

In using the X^2 and ANOVA tests, groupings of the data presented in Table 8 were assumed to be representative of the same "true" population. This hypothesis, as represented by the calculated variances and means, was then tested by comparing the calculated $X^2_{(x)}$ and $F_{(x)}$ values to those of hypothetical, normally distributed, groups of data. The results for coated and uncoated samples are shown in Table 9.

To interpret the table, compare the calculated $X^2_{(x)}$ and $F_{(x)}$ values to those of the predicted $X^2_{(0.05)}$ and $F_{(0.05)}$ values. The groupings being tested are considered to be statistically indistinguishable (within defined confidence limits) if $X^2_{(x)}$ $X^2_{(0.05)}$ and $F_{(x)}$ $F_{(0.05)}$. The 0.05 significance level was used for both the X^2 and ANOVA (F) reference populations. This significance level results in 95% confidence in the indications of the X^2 test and 90% confidence in the ANOVA (the ANOVA tested only one tail of the population-frequency distribution; hence, the confidence level is reduced).

The results (Table 9) indicate the stated hypothesis is valid with respect to the variances in all cases. The table also shows the hypothesis to be valid for the means in 14 of the 18 tested cases. Of the four ANOVA tests which failed, two were in the control groups (0 cycles), indicating that the inherent material variability is more significant than the degradation produced by the environmental conditioning. Of the other two tests which failed, one showed significant deviation (both higher and lower) from the pooled mean only for the 52- and 53-cycle samples in the uncoated middle groups. The remaining test which failed (coated middle groups) resulted from 7- and 37-cycle samples being lower, and 52- and 53-cycle samples being higher than the pooled mean. Again, the deviation from the expected values could not be clearly attributed to the freeze/thaw environment.

Table 8. Modulus of Rupture (p.s.i.)

Uncoated Specimens

		Number of Cycles				
		0	7	38	52	53
TOP (A,E)	N	4	4	4	4	4
	MEAN	105.5	102.6	89.3	108.8	95.5
	STD.	4.224	12.227	12.768	6.168	19.370
	C.V.	0.0400	0.1191	0.1429	0.0566	0.2027
MID (B,C,F,G)	N	8	8	8	8	8
	MEAN	100.1	100.2	99.5	106.5	98.6
	STD.	3.668	6.799	5.194	5.695	7.151
	C.V.	0.0366	0.0678	0.0522	0.0534	0.0725
BOT (D,H)	N	4	4	4	4	4
	MEAN	97.6	103.8	102.6	105.8	96.7
	STD.	1.556	8.026	6.429	4.328	7.066
	C.V.	0.0159	0.0773	0.0626	0.0408	0.0730

Coated Specimens

		0	7	38	52	53
TOP (A,E)	N	4	4	4	4	4
	MEAN	100.9	107.5	104.5	107.7	112.5
	STD.	13.599	8.756	10.861	6.300	6.691
	C.V.	0.1347	0.0814	0.1038	0.0584	0.0594
MID (B,C,F,G)	N	8	8	8	8	8
	MEAN	99.9	93.8	93.4	106.7	104.6
	STD.	8.826	10.992	8.254	7.712	9.215
	C.V.	0.0882	0.1170	0.0883	0.0722	0.0880
BOT (D,H)	N	4	4	4	4	4
	MEAN	115.7	101.3	108.9	119.8	110.1
	STD.	5.131	8.543	15.109	11.861	6.206
	C.V.	0.0443	0.0842	0.1387	0.0990	0.0563

Note: N - Sample Number
MEAN - Sample Mean
STD. - Standard Deviation
C.V. - Coefficient of Variation

Table 9. Comparison of Test Results (MOR)

Property	Sample	Conditioning (No. of Cycles)	Cal^c $X^2(x)$	Predict $X^2(0.05)$	Cal^c F(x)	Predict F(0.05)
Modulus of Rupture (Uncoated)	TOP(A,E)	All	6.32	9.49	1.67	3.06
	MID(B,C,F,G)	All	3.29	9.49	4.59	2.64
	BOT(D,H)	All	5.87	9.49	0.18	1.78
	All	0	2.43	5.99	5.58	3.80
	All	7	1.47	5.99	0.27	3.80
	All	38	3.63	5.99	2.53	3.80
	All	52	0.35	5.99	0.32	3.80
	All	53	5.15	5.99	0.11	3.80
	All	52,53	11.03	11.07	1.38	2.77
Modulus of Rupture (Coated)	TOP(A,E)	All	2.22	9.49	0.55	3.06
	MID(B,C,F,G)	All	0.99	9.49	3.60	2.64
	BOT(D,H)	All	3.98	9.49	1.96	3.06
	All	0	2.35	5.99	3.97	3.80
	All	7	0.33	5.99	2.62	3.80
	All	38	1.52	5.99	3.20	3.80
	All	52	1.26	5.99	3.30	3.80
	All	53	0.72	5.99	1.44	3.80
	All	52,53	2.05	11.07	2.13	2.77

Further examination of Table 9 reveals that both the X^2 and ANOVA tests pass for the pooled sample of 52 and 53 cycles with respect to all specimen locations. Since the 52- and 53-cycle groups were taken at the same time and from all levels within the chamber, the possible effect of chamber location on weathering, and possible discrepancies in the time rate-of-change of materials properties, are shown to be negligible.

As a result of the X^2 and ANOVA tests, it was concluded that the variation observed in the means of MOR sample groups was a result of factors other than freeze/thaw conditioning. Figures 38 and 39 illustrate the pooled coated and uncoated MOR samples, respectively, in histogram form. Descriptive statistics are included for the uncoated sample in Figure 39.

It was postulated that perhaps the observed variations of the MOR values could be related to slight density variations. Linear regression techniques were used to evaluate the relation of MOR to density for all conditioning levels of uncoated Foamglas . The resultant distribution of the pooled samples is shown in Figure 40 along with the fitted linear regression line. The correlation and linear regression statistics for the distribution are shown in Table 10.

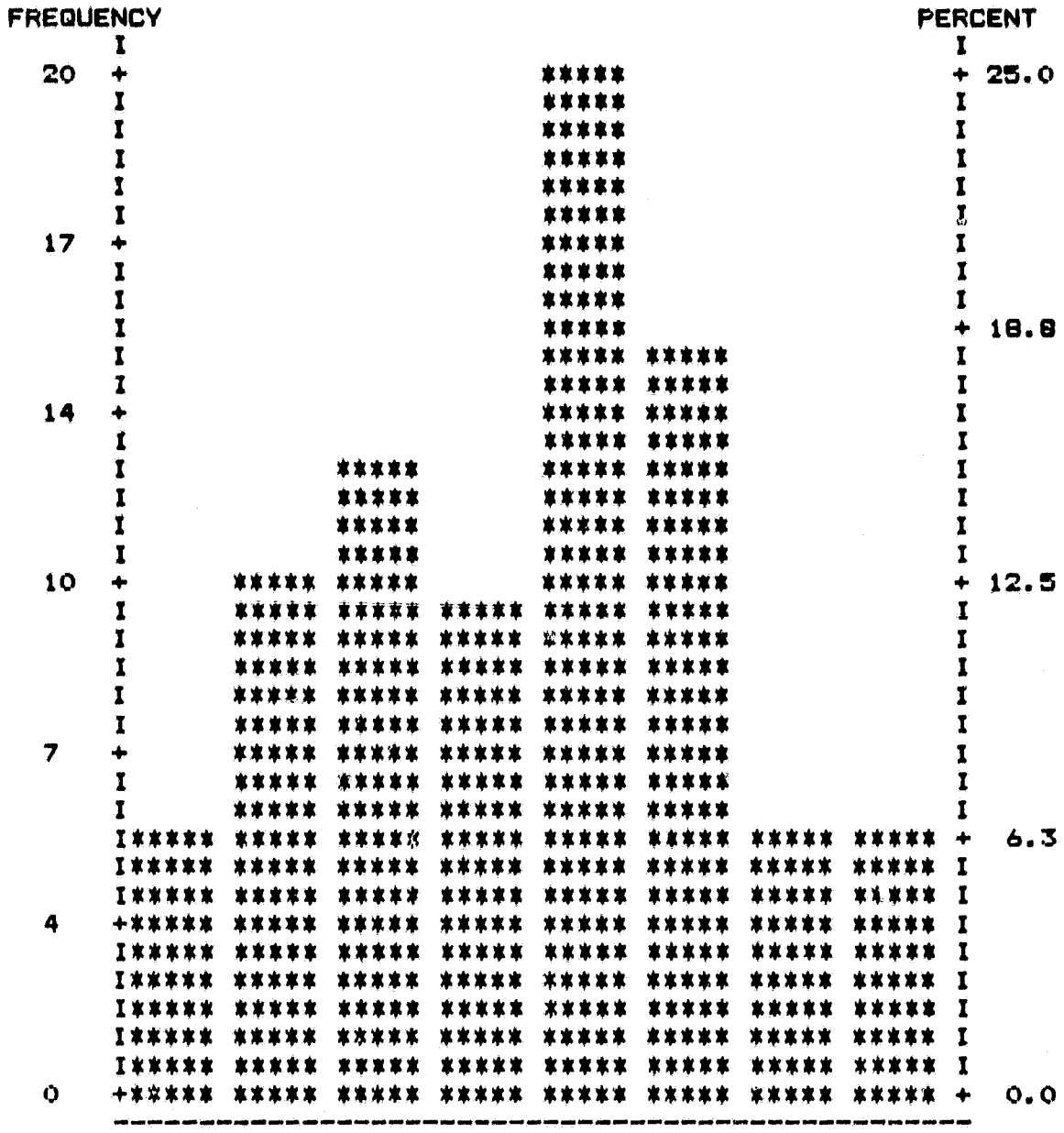

Figure 38. Pooled, Coated MOR

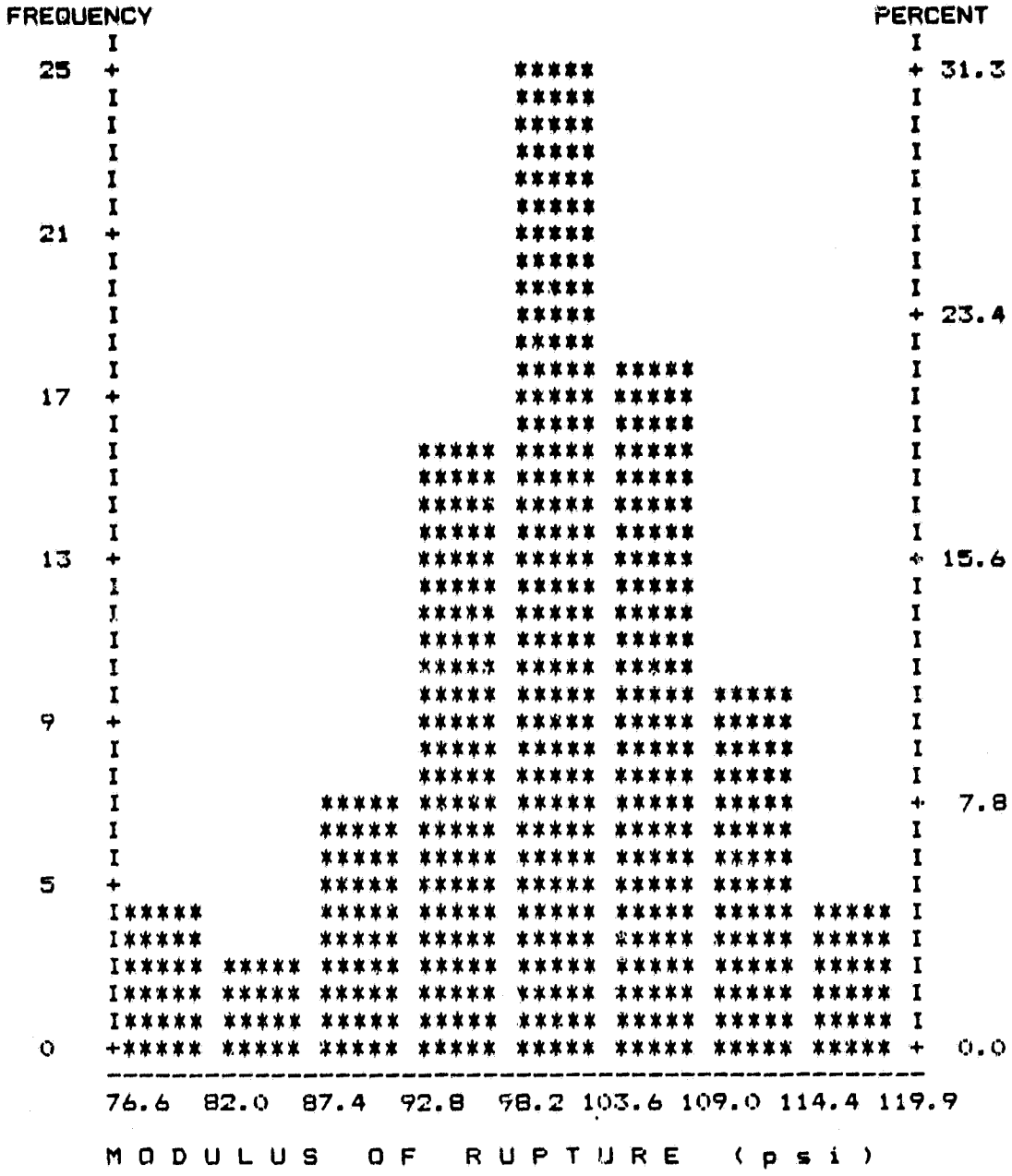

Mean:	100.9
Variance:	73.8
Standard Deviation:	8.6
Skewness:	-.659
Kurtosis:	.706

Figure 39. Pooled, Uncoated MOR

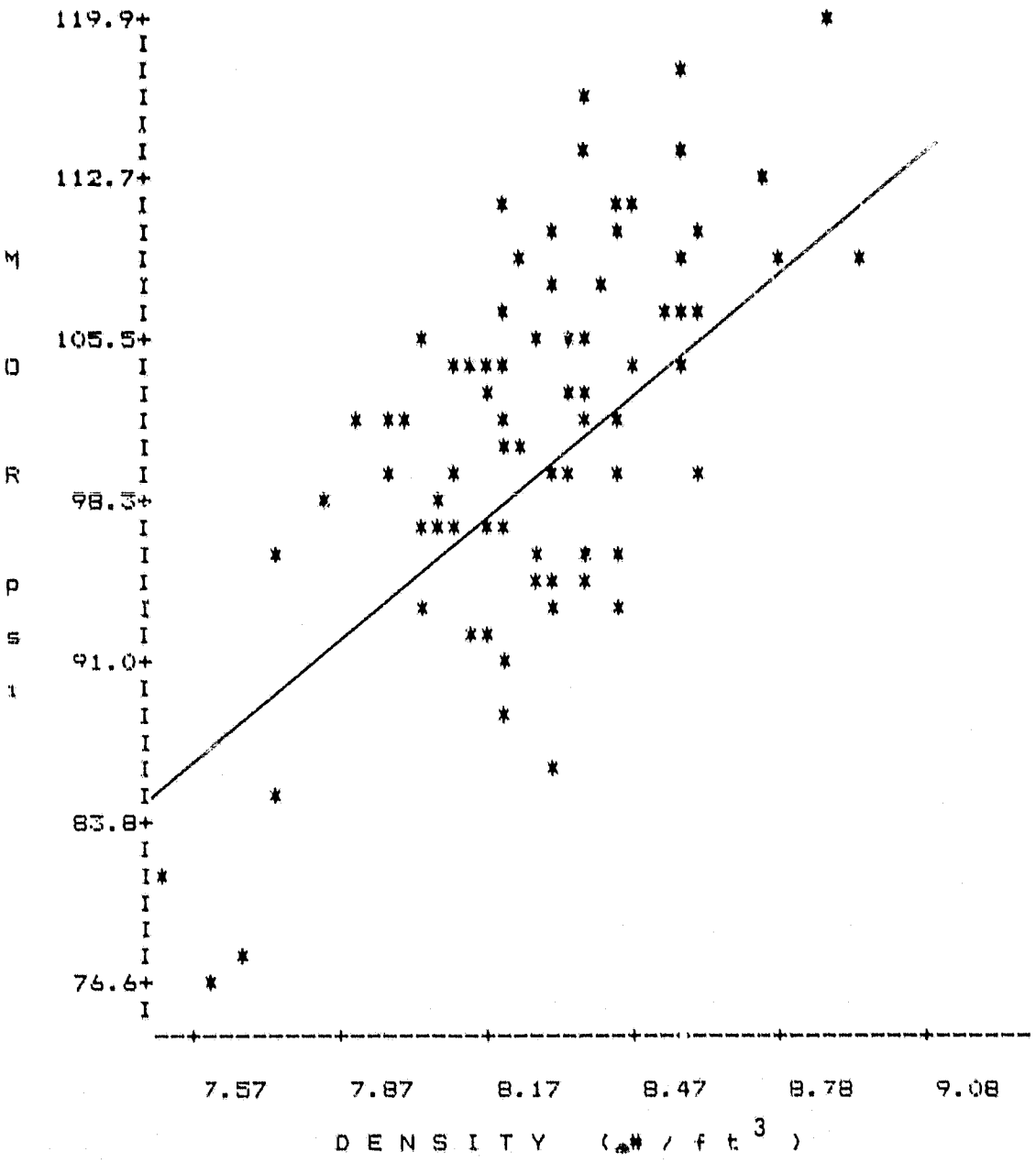

Figure 40. Uncoated MOR Versus Density

Table 10. Statistics for Pooled Uncoated MOR vs. Density

Mean density	8.38 lb/ft^3
Standard deviation of the mean density	0.29
Mean MOR	100.95 psi
Standard deviation of the mean MOR	8.36
Number of pairs of data	79
Correlation coefficient (R)	0.624
Slope (m) of regression line	18.25 psi
Y intercept (B) for regression line	-51.922 $psi/lb/ft^3$

The maximum value for the correlation coefficient (R) which may be expected to occur by chance alone (when actually no correlation exists) for a sample of 80 is 0.283 (assuming a 99% confidence level).[26] The observed R value, 0.624, indicates a 99+% probability that MOR variation correlates with density. The actual variability of MOR due to fluctuations of sample densities may be expressed as R^2. In this case, R^2 is 0.389, indicating that nearly 38.9% of the scatter of the MOR data is related to the observed sample density variation. Hence, mechanical properties are significantly influenced not only by the density variation, but also by variation in strength at a given density (suspected to be caused by microstructural variation).

Note that, while the sample was handled with reasonable care, the techniques used were representative of those which would be used in the actual fabrication environment, and thereby represent the variations which would be expected in field applications.

2. Young's Modulus (Modulus)

The same statistical approach and procedures were used for the evaluation of modulus as were used for MOR. Table 11 displays the statistics for the top, middle and bottom groups of coated and uncoated Foamglas modulus specimens with respect to cycle number. Again, inspection of the data did not reveal any trend of degradation with increasing cycles.

The X^2 and ANOVA tests were again used to test the hypothesis that the effect of weathering on modulus was indistinguishable from the natural variability found in the unconditioned material.

Table 12 lists the results of the X^2 (test of the variances) and ANOVA (test of the means) tests. Of the 18 X^2 tests, 14 passed, and all 18 of the ANOVA tests passed. Of the four failing X^2 tests, two (middle uncoated

Table 11. Young's Modulus (p.s.i.)

Uncoated Specimens

		Number of Cycles				
		0	7	38	52	53
TOP (A,E)	N	4	4	4	4	4
	MEAN	195681	208822	190159	186424	201913
	STD.	31648.5	7972.7	15715.0	17984.8	20789.1
	C.V.	0.161734	0.038179	0.082641	0.096472	0.102960
MID (B,C,F,G)	N	8	8	8	8	7
	MEAN	186857	199478	198055	193452	196046
	STD.	5233.2	14267.7	15290.4	6253.4	20399.2
	C.V.	0.028006	0.071525	0.077202	0.032325	0.104050
BOT (D,H)	N	4	4	4	4	4
	MEAN	177470	210854	191062	184402	195927
	STD.	11357.7	14885.4	15810.6	20112.4	16518.1
	C.V.	0.063998	0.070596	0.082751	0.109068	0.084307

Coated Specimens

		0	7	38	52	53
TOP (A,E)	N	4	4	4	4	4
	MEAN	172702	191537	173558	165943	176289
	STD.	17954.4	14821.9	15147.3	13632.5	19303.0
	C.V.	.103962	0.077383	0.087275	0.082157	0.109496
MID (B,C,F,G)	N	8	7	8	8	8
	MEAN	190028	173941	186229	187589	194126
	STD.	14614.3	11953.2	16773.0	15408.7	17798.9
	C.V.	.076904	0.068720	0.090066	0.082140	0.091687
BOT (D,H)	N	3	4	4	4	4
	MEAN	180314	171381	168716	190751	194047
	STD.	1652.7	21518.4	27193.9	27545.7	17649.1
	C.V.	0.009166	0.125558	0.161181	0.144406	0.090952

Note:
N - Sample Number
MEAN - Sample Mean
STD. - Standard Deviation
C.V. - Coefficient of Variation

Table 12. Comparison of Test Results (Modulus)

Property	Sample	Conditioning (No. of Cycles)	Calc $X^2(x)$	Predict $X^2(0.05)$	Calc F(x)	Predict F(0.05)
Young's Modulus (Uncoated)	TOP(A,E)	All	4.52	9.49	0.78	3.06
	MID(B,C,F,G)	All	14.74	9.49	0.37	2.65
	BOT(D,H)	All	0.85	9.49	2.51	3.06
	All	0	12.99	5.99	1.20	3.80
	All	7	1.16	5.99	1.25	3.80
	All	38	0.01	5.99	0.46	3.80
	All	52	6.36	5.99	2.27	3.80
	All	53	0.18	5.99	0.13	3.88
	All	52,53	8.03	11.07	1.87	2.77
Young's Modulus (Coated)	TOP(A,E)	All	0.47	9.49	1.35	3.06
	MID(B,C,F,G)	All	1.01	9.49	1.74	2.65
	BOT(D,H)	All	8.09	9.49	1.04	3.11
	All	0	6.20	5.99	1.91	3.88
	All	7	1.34	5.99	2.11	3.88
	All	38	1.29	5.99	1.27	3.80
	All	52	1.91	5.99	2.27	3.80
	All	53	0.03	5.99	1.45	3.80
	All	52,53	1.97	11.07	1.61	2.77

samples at all conditioning levels and uncoated samples at all locations with 52 cycle conditioning levels) were driven to failure by abnormally narrow scatter (small sample variance). This would certainly not be expected to be the result of weathering, especially considering the fact that the abnormal samples were 0 and 52 cycles. Of the remaining two failures (coated and uncoated controls at all levels), both were again caused by abnormally narrow scatter. This might be expected of the controls, if all samples were from similar locations. However, one group was from the bottom (coated), and one was from the middle (uncoated). Again, inherent material variability and the expected effects of normal "random sampling" produced by specimen selection appear to be the main causes of variations within the measured properties.

Again the combined groups of 52 and 53 cycles passed the X^2 and ANOVA tests for coated and uncoated specimens at all locations, indicating that chamber location had no effect upon the calculated modulus values.

Histograms of the pooled coated and uncoated modulus samples are shown, along with the descriptive statistics for the uncoated specimens, in Figures 41 and 42. Once again, it appears that the data represents a normal distribution.

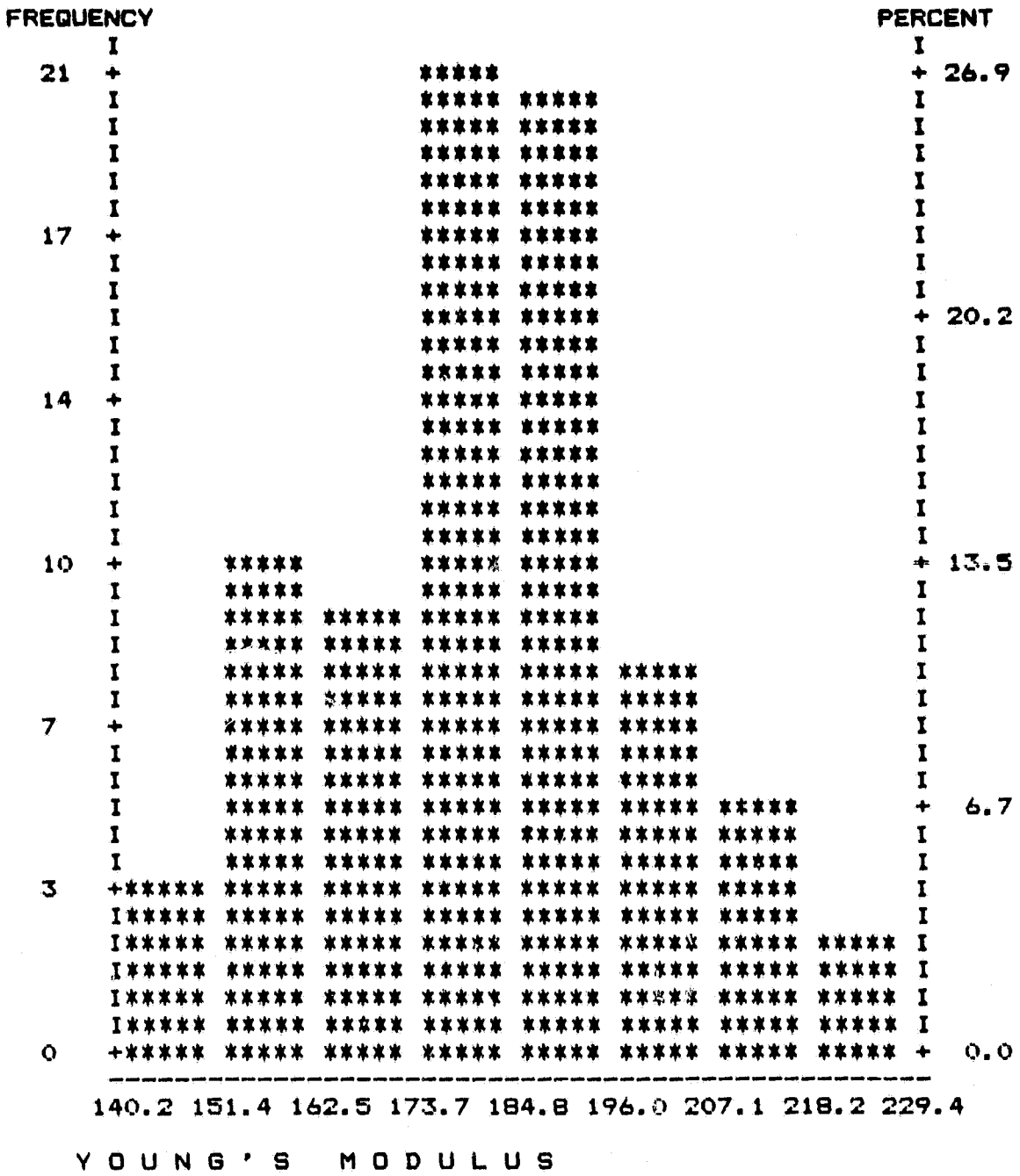

Figure 41. Pooled, Coated Modulus

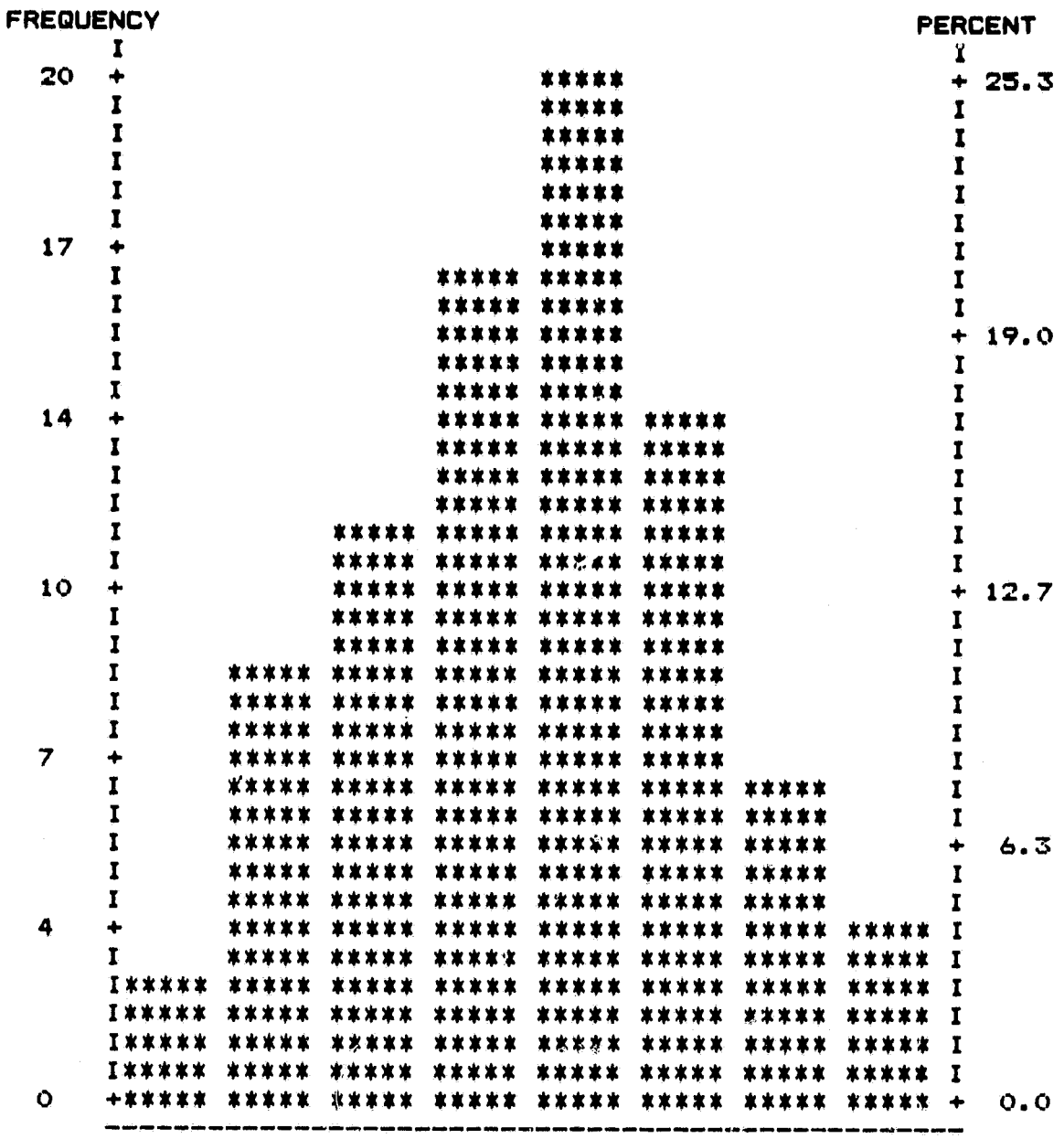

Mean:	194.5 KSI
Variance:	265.0
Standard Deviation:	16.3
Skewness:	.004
Kurtosis:	-0.[illegible]

Figure 42. Pooled, Uncoated Modulus

The variation of modulus values as a function of density was again evaluated using linear regression techniques. The resultant distribution of the pooled samples is shown in Figure 43, along with the best fit regression line. The correlation and linear regression statistics for the distribution are shown in Table 13.

The correlation coefficient (R) indicates a 99+% probability that modulus variation was correlated with density. The actual variability (R^2) attributable to density fluctations is 0.294 (or 29.4%), once again indicating that microstructure significantly contributes to the observed variability of the mechanical properties at any given density.

Table 13. Statistics for Pooled Uncoated Modulus vs. Density

Mean density	8.37 lb/ft^3
Standard deviation of the mean density	0.28
Mean modulus	194.5 KSI
Standard deviation of the mean modulus	16.3
Number of pairs of data	79
Correlation coefficient (R)	0.542
Slope (m) of regression line	31.5 $ksi/lb/ft^3$
Y intercept (B) for regression line	-69.1 ksi

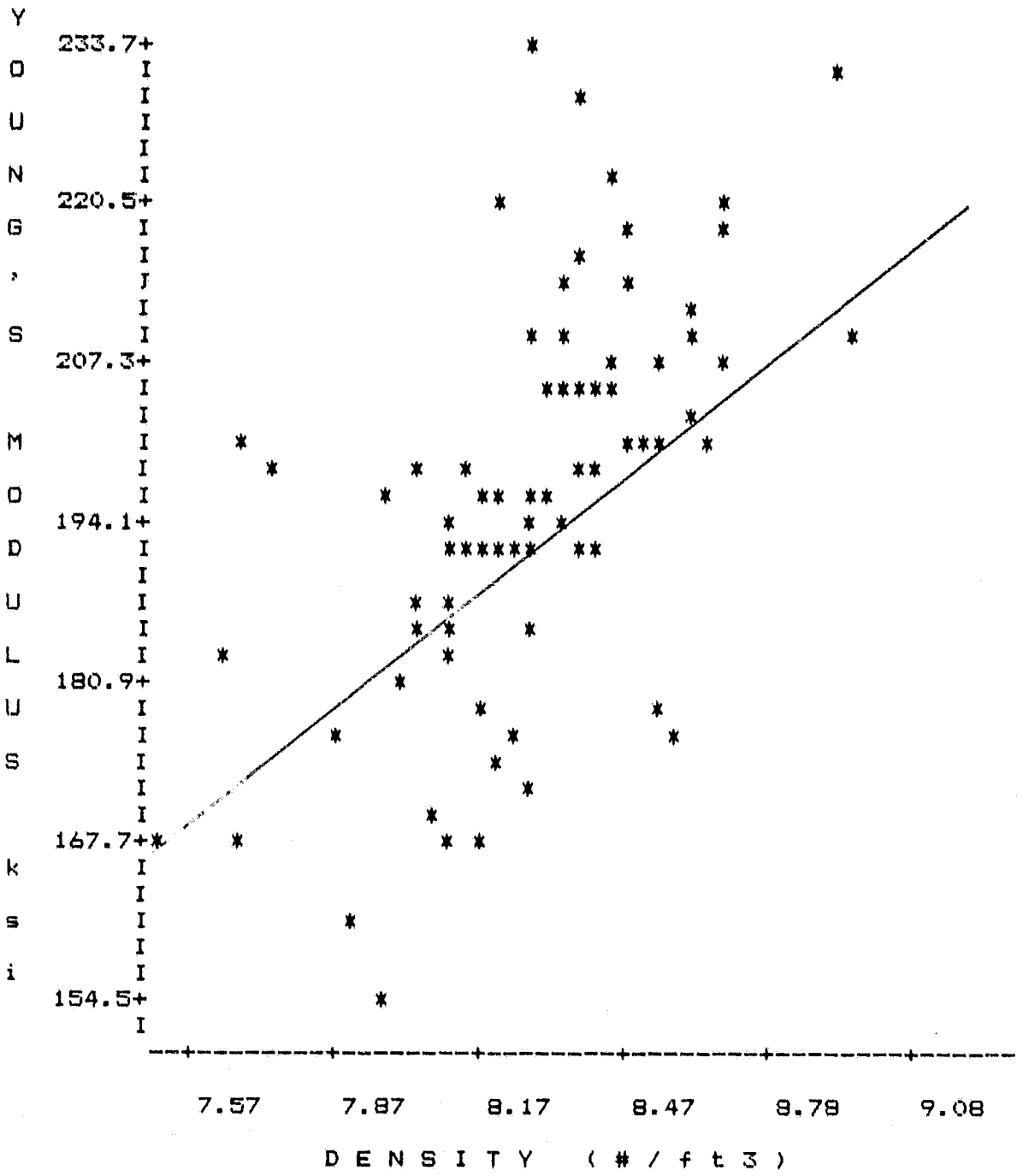

Figure 43. Uncoated Modulus Versus Density

SECTION VIII

SUMMARY AND CONCLUSIONS

No degradation of physical or mechanical properties, including density, Modulus of Rupture, or Young's Modulus, was observed after 53 freeze/thaw cycles.

Basic inherent material variability, unrelated to freeze/thaw effects, appeared to be the major contributer to variations observed within the results. No significant variation in the above specimen properties was noted relative to freeze/thaw cycle number, specimen parent block location (top, middle or bottom of block), location within the chamber, or coated or uncoated preparation.

No significantly different behavior between the coated and uncoated Foamglas® was observed relative to the measured materials properties. However, if significantly more than 53 freeze/thaw cycles are expected in field applications, a protective conformal coating may be required. Additional testing is required to establish this.

Cellular glass freeze/thaw test results are highly dependent upon test design, specifically the time/temperature/humidity cycle, chamber and specimen geometry, sampling method and sample preparation.

SECTION IX

RECOMMENDATIONS

The following general recommendations are based upon the insight gained from this study. If implemented, they would allow a more straightforward evaluation and optimization of specific designs with respect to freeze/thaw effects:

(1) Establish realistic standard freeze/thaw cycle(s), testing procedure(s), and evaluation criteria for structural mirror-backing substrates of solar collectors. This must be based on better understanding of actual freeze/thaw meteorological conditions, their frequency, etc.

(2) Determine the time rate-of-change of materials properties for the appropriate cycle(s) above for various mirror-backing materials.

(3) Evaluate any candidate conformal coatings with the methods determined in (1) and the results from (2).

(4) Investigate the effect upon degradation rate of flat, concave and convex specimen designs in horizontal, inclined and vertical orientations.

The freeze/thaw cycle presented in this paper satisfies part of recommendation (1). However, the testing procedure, evaluation criteria, specimen and chamber geometry, and recommendations (2) through (4), would be design-specific, and, therefore, must be addressed on an individual basis.

REFERENCES

1. Giovan, M., and Adams, M., Evaluation of Cellular Glasses for Solar Mirror Panel Applications, DOE/JPL-1060-24, June 15, 1979.

2. Oakeson, W. G., et al., Foam Glass Insulation From Waste Glass, Utah University, Salt Lake City, Utah, August 1977.

3. Zwissler, J., Fracture Mechanics of Cellular Glass, in print.

4. Technical Brochures, Various, Pittsburgh Corning.

5. Lovett, W., Foamglas® Ice Rink Specifications, Pittsburgh Corning Corp., Technical Literature #TD-76, April 2, 1973.

6. Zwissler, J., Environmental Susceptibility of Cellular Glass Materials, JPL IOM 354/JZ/020, January 29, 1979.

7. Argoud, M. J., Test Bed Concentrator Mirrors, DOE/JPL 1060-33, January 1980.

8. Giovan, M. N., Foamglas® Mirror Facet, JPL IOM 354/MG/100, August 18, 1978.

9. Allred, R. E., Evaluation of Cellular Glass for Solar Reflector Structures, Sandia IOM, December 21, 1978.

10. Miller, D., and Beauchamp, E., Private Communication, January 1981.

11. Allred, R. E., Private Communication, January 1981.

12. Carpenter, R., and Cleland, E., Initial Report on Studies of Conformal Coating for Cellular Glass, JPL IOM 354/EC/093, May 14, 1979.

13. Giovan, M., Foamglas® Freeze/Thaw Testing, JPL IOM 354/MG/111, May 23, 1979.

14. Hasegawa, T., Failure Analysis - Mirror Glass/Foamglas® Bonded Panels, Flat Configuration, JPL IOM 354/TH/122, June 12, 1979.

15. McMarlin, R., Freeze/Thaw Damage of Foamglas® Insulation, Pittsburgh Corning Technical Information Letter TD-141, September 4, 1979.

16. Meyer, G., and McMarlin, R., Water Durability of Foamglas® Insulation, Pittsburgh Corning Technical Information Letter TD-141, September 27, 1979.

17. Rostoker, D., Specialty Cellular Glass Products and Their Applications, Pittsburg Corning Corporation.

18. Foamglas® Insulation 20 Year Performance, Pittsburgh Corning Corp., January 1979.

19. Berry, M., Private Communication, January 1981.

20. Wischmann, K. B., and Gonzales, M. H., Protective Coatings and Sealants for Solar Applications, SAND 80-0808, September 1980.

21. Kaplar, C. W., Moisture and Freeze/Thaw Effects on Rigid Thermal Insulations, Cold Regions Research and Engineering Laboratory, Hanover, New Hampshire, April 1974.

22. Cleland, E., and Adams, M., Private Communication, November 1980.

23. Hedlin, C. P., Moisture Gains by Foam Plastic Roof Insulations Under Controlled Temperature Gradients, Journal of Cellular Plastics, September/October, 1977.

24. Myers, R., and Long, J., Treatise on Coatings, Vol 2, Characterization of Coatings: Physical Techniques, Part I, pp. 142-144, 1969.

25. Volk, W., Industrial Statistics, Chemical Engineering, March 1956.

26. Lipson, C., and Sheth, N. J., Statistical Design and Analysis of Engineering Experiments, McGraw-Hill, 1973.

APPENDIX A

FOAMGLAS® FREEZE/THAW DATA BASE FILE

APPENDIX A

*** FOAMGLAS® FREEZE/THAW ***
Data Base File

PB	ID	LOAD	DEFLECT	WIDTH	HEIGHT	LENGTH	MASS	MOR	MODULUS	DENSITY	C	CYC
A-8	A	9.224	0.0325	2.492	0.936	17.95	133.1	99.9	183132		Y	0
A-8	B	10.220	0.0312	2.477	0.996	17.95	112.6	97.4	175335		Y	0
A-8	C	9.351	0.0296	2.474	0.971	17.95	110.0	95.4	185496		Y	0
A-8	D	10.600	0.0376	2.480	0.931	17.95	126.6	113.7	181405		Y	0
A-8	E	12.150	0.0360	2.448	0.966	17.95	134.7	120.4	193999		Y	0
A-8	F	10.920	0.0320	2.442	0.984	17.95	111.8	107.0	190298		Y	0
A-8	G	10.710	0.0301	2.453	0.947	17.95	112.0	113.3	222975		Y	0
A-8	H	11.510	0.0000	2.469	0.932	17.95	128.0	122.5	0		Y	0
A-9	A	7.735	0.0341	0.431	0.931	17.95	124.5	90.0	157269		Y	0
A-9	B	9.406	0.0341	2.438	0.984	17.95	108.1	94.8	177151		Y	0
A-9	C	10.880	0.0336	2.443	0.971	17.95	110.8	109.9	188377		Y	0
A-9	D	10.740	0.0389	2.440	0.934	17.95	131.3	116.3	178413		Y	0
A-9	E	8.504	0.0352	2.516	0.932	17.95	131.3	93.5	158407		Y	0
A-9	F	8.649	0.0272	2.511	0.962	17.95	107.3	89.8	191818		Y	0
A-9	G	9.454	0.0277	2.506	0.986	17.95	109.7	92.1	188771		Y	0
A-9	H	10.680	0.0360	2.503	0.945	17.95	133.5	110.3	181126		Y	0
A-19	A	9.739	0.0360	2.434	0.969	17.95	88.5	100.7	160868	7.959	N	0
A-19	B	10.340	0.0309	2.442	0.981	17.95	93.2	102.8	189774	8.247	N	0
A-19	C	10.360	0.0325	2.442	0.986	17.95	93.4	102.1	178102	8.227	N	0
A-19	D	9.139	0.0325	2.454	0.955	17.95	87.5	97.7	175534	7.921	N	0
A-19	E	9.424	0.0280	2.480	0.918	17.95	89.8	107.3	233724	8.369	N	0
A-19	F	11.080	0.0304	2.481	1.008	17.95	95.4	101.7	186159	8.091	N	0
A-19	G	10.210	0.0277	2.469	1.005	17.95	95.9	96.1	193718	8.200	N	0
A-19	H	9.842	0.0325	2.467	0.977	17.95	94.0	98.7	173570	8.275	N	0
A-20	A	9.557	0.0333	2.374	0.959	17.95	88.0	103.7	181020	8.195	N	0
A-20	B	9.454	0.0296	2.376	0.991	17.95	90.0	96.3	183677	8.108	N	0
A-20	C	9.878	0.0328	2.389	0.969	17.95	89.5	103.8	182310	8.198	N	0
A-20	D	8.970	0.0328	2.404	0.969	17.95	85.8	95.4	167142	7.812	N	0
A-20	E	10.340	0.0320	2.522	0.932	17.95	94.5	110.4	207114	8.527	N	0
A-20	F	9.279	0.0388	2.503	0.965	17.95	95.2	95.0	191192	8.363	N	0
A-20	G	11.530	0.0301	2.487	1.016	17.95	97.4	103.3	189924	8.179	N	0
A-20	H	8.897	0.0304	2.474	0.936	17.95	89.3	98.7	193637	8.183	N	0
A-10	A	10.080	0.0330	2.456	0.952	17.97	129.5	110.1	195805		Y	7
A-10	B	10.690	0.0370	2.450	0.988	17.97	106.0	108.3	165371		Y	7
A-10	C	8.651	0.0290	2.452	0.993	17.97	105.2	90.7	175827		Y	7
A-10	D	7.520	0.0390	2.445	9.320	17.97	123.2	92.1	140299		Y	7
A-10	E	7.905	0.0270	2.447	0.937	17.97	127.2	94.5	208375		Y	7
A-10	F	8.165	0.0000	2.444	1.000	17.97	107.4	85.8	0		Y	7
A-10	G	7.929	0.0260	2.442	1.002	17.97	105.7	83.4	178334		Y	7
A-10	H	7.638	0.0330	2.448	0.917	17.97	121.2	96.1	176391		Y	7
A-6	A	9.646	0.0360	2.454	0.924	17.95	133.6	113.0	189190		Y	7
A-6	B	6.537	0.0300	2.447	0.942	17.95	106.7	82.0	160957		Y	7
A-6	C	7.881	0.0280	2.423	0.955	17.95	105.4	91.7	191129		Y	7
A-6	D	7.929	0.0360	2.450	0.877	17.95	127.8	108.0	189803		Y	7
A-6	E	9.036	0.0400	2.454	0.903	17.95	131.4	112.4	172780		Y	7
A-6	F	9.362	0.0360	2.453	0.926	17.95	103.9	110.8	185134		Y	7
A-6	G	7.822	0.0370	2.455	0.917	17.95	104.1	98.4	160838		Y	7
A-6	H	8.396	0.0380	2.451	0.891	17.95	128.5	109.2	179034		Y	7

PB	ID	LOAD	DEFLECT	WIDTH	HEIGHT	LENGTH	MASS	MOR	MODULUS	DENSITY	C
A-16	A	9.474	0.0310	2.433	0.943	17.90	97.9	108.8	207878	9.080	N
A-16	B	9.048	0.0290	2.431	0.940	17.90	94.2	105.7	216688	8.771	N
A-16	C	8.929	0.0320	2.442	0.966	17.90	95.6	98.6	177845	8.625	N
A-16	D	8.302	0.0280	2.440	0.955	17.90	93.9	95.5	199298	8.588	N
A-16	E	8.006	0.0290	2.440	0.904	17.90	91.1	103.7	220355	8.789	N
A-16	F	8.533	0.0260	2.441	0.980	17.90	96.3	92.6	203233	8.568	N
A-16	G	9.196	0.0290	2.441	0.949	17.90	93.3	104.6	212473	8.579	N
A-16	H	10.630	0.0320	2.434	0.978	17.90	95.3	110.8	198177	8.529	N
A-18	A	7.366	0.0240	2.418	0.971	17.97	92.5	85.2	204140	8.350	N
A-18	B	8.017	0.0290	2.418	0.964	17.97	90.0	92.1	183567	8.195	N
A-18	C	9.237	0.0310	2.420	0.953	17.97	88.3	105.0	198385	8.120	N
A-18	D	7.822	0.0260	2.428	0.922	17.97	89.2	98.4	229169	8.444	N
A-18	E	9.900	0.0330	2.431	0.942	17.97	93.4	112.9	202917	8.662	N
A-18	F	8.882	0.0250	2.431	0.991	17.97	95.3	92.7	212126	8.386	N
A-18	G	10.100	0.0330	2.428	0.966	17.97	92.5	109.3	191508	8.356	N
A-18	H	8.983	0.0310	2.423	0.918	17.97	89.6	110.6	216774	8.536	N
A-2	A	10.730	0.0350	2.507	0.953	17.90	136.4	108.8	182266		Y
A-2	B	10.110	0.0265	2.446	1.017	17.90	113.1	93.9	195888		Y
A-2	C	10.470	0.0295	2.440	1.028	17.90	112.1	94.9	175505		Y
A-2	D	8.100	0.0390	2.415	0.933	17.90	127.1	93.6	142637		Y
A-2	E	7.209	0.0337	2.309	0.932	17.90	125.4	89.5	157780		Y
A-2	F	6.700	0.0280	2.288	0.949	17.90	97.8	83.1	173687		Y
A-2	G	8.974	0.0300	2.314	1.025	17.90	106.2	88.6	160967		Y
A-2	H	8.695	0.0340	2.352	0.940	17.90	130.7	100.2	174467		Y
A-4	A	10.270	0.0372	2.485	0.957	17.85	137.6	104.9	164083		Y
A-4	B	7.597	0.0255	2.487	0.960	17.85	112.4	82.3	187658		Y
A-4	C	10.920	0.0297	2.465	1.024	17.85	118.8	98.1	180725		Y
A-4	D	10.320	0.0450	2.478	0.920	17.85	137.3	114.3	153398		Y
A-4	E	10.390	0.0365	2.449	0.925	17.85	134.6	115.0	190104		Y
A-4	F	10.500	0.0272	2.453	0.994	17.85	117.7	101.2	210036		Y
A-4	G	11.280	0.0287	2.467	1.002	17.85	118.1	105.2	205372		Y
A-4	H	12.050	0.0375	2.472	0.931	17.85	138.1	127.5	204363		Y
A-12	A	8.610	0.0280	2.482	0.953	17.90	93.5	92.5	193571	8.413	N
A-12	B	9.901	0.0312	2.487	0.984	17.90	95.8	97.0	176410	8.331	N
A-12	C	11.770	0.0290	2.476	1.025	17.90	98.7	103.8	196682	8.277	N
A-12	D	10.710	0.0330	2.481	0.950	17.90	94.9	111.4	198804	8.569	N
A-12	E	10.370	0.0302	2.386	0.980	17.90	94.7	105.9	200230	8.619	N
A-12	F	9.700	0.0265	2.385	1.015	17.90	96.8	93.5	195044	8.510	N
A-12	G	9.000	0.0280	2.385	0.957	17.90	94.7	98.9	206420	8.830	N
A-12	H	9.622	0.0292	2.394	0.962	17.90	92.0	103.0	204829	8.502	N
A-14	A	7.112	0.0287	2.490	0.941	17.90	83.3	81.3	167033	7.566	N
A-14	B	10.010	0.0290	2.493	0.978	17.90	92.1	98.9	195328	8.039	N
A-14	C	9.180	0.0305	2.485	0.903	17.90	87.5	108.3	219688	8.299	N
A-14	D	10.100	0.0320	2.482	0.997	17.90	94.6	96.3	168707	8.136	N
A-14	E	6.051	0.0235	2.427	0.918	17.90	80.9	77.5	199803	7.728	N
A-14	F	8.658	0.0300	2.430	0.962	17.90	89.1	93.1	179958	8.112	N
A-14	G	9.568	0.0280	2.435	0.954	17.90	92.0	102.5	214914	8.429	N
A-14	H	9.562	0.0302	2.448	0.963	17.90	91.4	100.0	191910	8.252	N
A-1	A	12.280	0.0388	2.481	0.988	17.99	141.8	114.5	167058		Y
A-1	B	11.340	0.0295	2.468	0.982	17.95	117.0	109.6	212502		Y
A-1	C	12.100	0.0368	2.468	0.991	17.96	117.6	114.1	175135		Y
A-1	D	12.560	0.0383	2.463	0.949	17.85	133.9	127.3	195967		Y
A-1	E	11.720	0.0390	2.465	0.987	17.95	135.7	110.9	160930		Y

PB	ID	LOAD	DEFLECT	WIDTH	HEIGHT	LENGTH	MASS	MOR	MODULUS	DENSITY	C	CYC
A-1	F	11.000	0.0330	2.466	1.004	17.95	113.0	102.5	173205		Y	52
A-1	G	11.580	0.0325	2.478	1.005	17.95	113.7	106.2	182316		Y	52
A-1	H	12.080	0.0365	2.476	0.938	17.90	134.0	125.4	204987		Y	52
A-3	A	10.600	0.0330	2.460	0.971	17.92	134.0	105.5	184073		Y	52
A-3	B	11.400	0.0306	2.412	1.008	17.92	110.7	107.1	194915		Y	52
A-3	C	10.930	0.0300	2.443	1.003	17.93	110.9	103.0	192017		Y	52
A-3	D	10.240	0.0388	2.459	0.973	17.90	130.5	[illegible]	150552		Y	52
A-3	E	9.100	0.0388	2.420	0.944	17.90	121.8	[illegible]	151714		Y	52
A-3	F	17.100	0.0293	2.411	1.143	17.92	130.6	[illegible]	202165		Y	52
A-3	G	10.100	0.0300	2.388	1.032	17.90	112.9	93.2	168463		Y	52
A-3	H	[illegible].000	0.0343	2.365	0.961	17.82	129.2	124.4	211499		Y	52
A-11	A	[illegible].720	0.0343	2.475	0.977	17.94	99.1	105.6	176140	8.699	N	52
A-11	B	11.220	0.0325	2.467	0.968	17.94	99.2	112.0	199480	8.815	N	52
A-11	C	12.180	0.0348	2.460	0.983	17.94	98.3	116.7	191232	8.622	N	52
A-11	D	9.500	0.0345	2.466	0.919	17.94	92.5	108.4	190572	8.666	N	52
A-11	E	10.000	0.0345	2.399	0.982	17.94	92.8	101.8	167689	8.364	N	52
A-11	F	10.080	0.0313	2.409	0.966	17.94	93.4	105.3	194593	8.513	N	52
A-11	G	10.200	0.0325	2.406	0.975	17.89	92.7	104.6	184417	8.409	N	52
A-11	H	10.020	0.0333	2.401	0.942	17.89	88.0	110.5	196607	8.276	N	52
A-13	A	11.400	0.0345	2.463	0.962	17.90	94.1	115.1	194131	8.445	N	52
A-13	B	11.280	0.0318	2.464	0.990	17.90	97.6	107.7	191805	8.508	N	52
A-13	C	9.700	0.0295	2.463	0.954	17.92	93.2	102.4	203632	8.429	N	52
A-13	D	9.420	0.0315	2.470	0.936	17.94	90.8	103.5	195923	8.336	N	52
A-13	E	11.200	0.0313	2.428	0.972	17.94	93.6	112.7	207736	8.415	N	52
A-13	F	9.200	0.0305	2.422	0.961	17.94	90.0	98.2	187148	8.208	N	52
A-13	G	9.620	0.0370	2.417	0.944	17.94	89.0	105.7	195312	8.276	N	52
A-13	H	9.600	0.0378	2.425	0.963	17.92	88.5	101.1	154506	8.050	N	52
A-5	A	11.120	0.0433	2.493	0.953	17.94	133.8	112.6	151925		Y	53
A-5	B	10.980	0.0300	2.494	1.008	17.94	115.6	110.4	186305		Y	53
A-5	C	9.240	0.0275	2.500	0.969	17.93	111.1	93.8	197009		Y	53
A-5	D	9.420	0.0368	2.504	0.903	17.90	130.7	108.8	182089		Y	53
A-5	E	10.800	0.0388	2.447	0.915	17.90	130.3	121.4	190666		Y	53
A-5	F	11.560	0.0323	2.452	0.978	17.92	112.5	113.2	200928		Y	53
A-5	G	14.420	0.0338	2.447	1.083	17.92	123.3	112.0	172667		Y	53
A-5	H	8.160	0.0305	2.445	0.879	17.92	126.5	104.6	217262		Y	53
A-7	A	10.480	0.0358	2.464	0.967	17.91	132.8	105.3	169715		Y	53
A-7	B	8.620	0.0273	2.458	0.983	17.91	110.7	87.7	182509		Y	53
A-7	C	10.000	0.0333	2.451	0.961	17.92	108.0	103.9	181340		Y	53
A-7	D	8.900	0.0375	2.448	0.895	17.92	122.6	108.0	178693		Y	53
A-7	E	11.360	0.0330	2.466	0.975	17.90	137.9	110.7	192851		Y	53
A-7	F	8.800	0.0300	2.460	0.887	17.90	102.1	109.6	229817		Y	53
A-7	G	12.600	0.0285	2.459	1.044	17.98	119.2	106.7	202438		Y	53
A-7	H	10.360	0.0370	2.465	0.905	17.98	129.4	119.0	198146		Y	53
A-15	A	9.240	0.0310	2.497	0.932	17.88	93.4	101.7	196457	8.548	N	53
A-15	B	9.720	0.0308	2.487	0.991	17.88	96.5	94.0	172079	8.333	N	53
A-15	C	9.020	0.0315	2.489	0.973	17.90	94.0	91.8	167103	8.260	N	53
A-15	D	7.640	0.0300	2.490	0.932	17.90	90.1	87.5	174081	8.258	N	53
A-15	E	9.880	0.0323	2.414	0.897	17.90	91.4	119.9	231187	8.978	N	53
A-15	F	10.120	0.0000	2.414	0.951	17.85	95.7	108.7	0	8.887	N	53
A-15	G	11.760	0.0293	2.419	1.008	17.85	100.0	109.6	208787	8.746	N	53
A-15	H	10.340	0.0278	2.428	0.993	17.85	97.8	101.1	205693	8.654	N	53
A-17	A	6.980	0.0255	2.460	0.925	17.80	83.0	83.9	197948	7.803	N	53
A-17	B	7.760	0.0288	2.474	0.924	17.85	88.8	90.8	190095	8.291	N	53

PB	ID	LOAD	DEFLECT	WIDTH	HEIGHT	LENGTH	MASS	MOR	MODULUS	DENSITY	C
A-17	C	8.840	0.0265	2.469	0.935	17.85	92.0	98.4	222194	8.495	N
A-17	D	8.600	0.0293	2.472	0.940	17.90	92.7	95.2	192670	8.483	N
A-17	E	6.700	0.0450	2.442	0.956	17.90	84.6	76.6	182061	7.708	N
A-17	F	8.280	0.0295	2.462	0.907	17.90	87.5	99.6	207387	8.334	N
A-17	G	9.060	0.0275	2.465	0.956	17.88	93.1	96.2	204682	8.410	N
A-17	H	8.500	0.0303	2.468	0.899	17.88	90.4	103.3	211267	8.675	N

Note:

PB - Parent Block
ID - Specimen Position
DEFLECT - Deflection [in.]
WIDTH - Block Width [in.]
HEIGHT [in.]
LENGTH [in.]
MASS [grams]
MOR - Modulus of Rupture [p.s.i.]
MODULUS - Youngs Modulus [p.s.i.]
DENSITY [lbs./cu.ft.]
C - Coated (Y/N)
CYC - Number of Freeze/Thaw Cycles